

**KERNFORSCHUNGSZENTRUM
KARLSRUHE**

Juni 1977

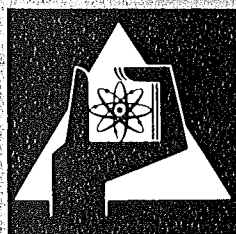
KFK 2456
EUR 5509e

Abteilung Behandlung radioaktiver Abfälle
Projekt Wiederaufarbeitung und Abfallbehandlung

**Long Term Leaching of Silicate Systems:
Testing Procedure, Actinides Behaviour and
Mechanism**

K. Scheffler, U. Riege

K. Louwrier, Hj. Matzke, I. Ray, H. Thiele
(Europäisches Institut für Transurane, Euratom)



**GESELLSCHAFT
FÜR
KERNFORSCHUNG M.B.H.
KARLSRUHE**

Als Manuskript vervielfältigt

Für diesen Bericht behalten wir uns alle Rechte vor

GESELLSCHAFT FÜR KERNFORSCHUNG M. B. H.
KARLSRUHE

KERNFORSCHUNGSZENTRUM KARLSRUHE

KFK 2456

EUR 5509e

PWA 14/77

Abteilung Behandlung Radioaktiver Abfälle
Projekt Wiederaufarbeitung und Abfallbehandlung

Long-Term Leaching of Silicate Systems:
Testing Procedure, Actinides Behaviour
and Mechanism

by

K. Scheffler

U. Riege

K. Louwrier⁺

Hj.Matzke⁺

I. Ray⁺

H. Thiele⁺

⁺) Europäisches Institut für Transurane,
Euratom

Gesellschaft für Kernforschung mbh, Karlsruhe

Abstract

Long-Term Leaching of Silicate Systems: Testing Procedure, Actinides Behaviour and Mechanism

High-level waste borosilicate glasses and medium-level waste cement products have been leached with various aqueous solutions at ambient temperature. The leach rates of americium and plutonium are determined as well as the behaviour of the actinides in the boundary surface glass/leachant and in the leachant itself. Methods like light-scattering photometry and differential refractometry, molecular filtration, scanning electron microscopy and α -spectrometry of the energy-loss of α -particles in thin layers have been applied.

From the experimental results a general model for the leaching mechanism has been established. A critical review of leach test procedures is accomplished aiming at the improvement of common tests with respect to the extrapolation of the obtained leach test data to final disposal safety considerations.

Zusammenfassung

Langzeitauslaugung von Silikat-Systemen: Bestimmungsmethode, Verhalten von Aktiniden und Mechanismus

Hochradioaktive Borosilikatgläser und mittelradioaktive Zementprodukte wurden mit verschiedenen wässrigen Lösungen bei Raumtemperatur ausgelaugt. Für Americium und Plutonium wurden die Auslaugraten bestimmt als auch das Verhalten der Aktiniden in der Phasengrenzfläche Glas/Auslaugmedium und im Auslaugmedium selbst. Angewendet wurden Meßtechniken wie Streulichtphotometrie und Differential-Refraktometrie, Molekularfiltration, Rasterelektronenmikroskopie und α -Spektrometrie über den Energieverlust von α -Teilchen in dünnen Schichten.

Aus den experimentellen Ergebnissen wird ein allgemeines Modell für den Auslaugmechanismus abgeleitet. Eine kritische Betrachtung von Auslaugtestverfahren wird mit dem Ziel durchgeführt, die bekannten Verfahren zu verbessern und eine Extrapolation der Auslaugtestergebnisse in Hinblick auf Sicherheitsbetrachtungen für die Endlagerung zu ermöglichen.

Résumé

Lixiviation à longue échéance des systèmes silicate: méthode d'essai, comportement des actinides et mécanisme

Des verres borosilicate à hautes activités et des produits de ciment à radioactivité modérée ont été lixiviés par des solutions aqueuses diverses à la température ambiante. Pour l'américium et pour le plutonium les coefficients de lixiviation sont déterminés ainsi que le comportement des actinides dans la couche limite entre le verre et la solution aqueuse et dans la solution de lixiviation. Les mesures ont été faites par photométrie des rayons lumineux diffusés et par réfractométrie, par filtration moléculaire, microscopie électronique et spectrométrie des particules alpha qui sont ralentis dans la surface lixiviée des verres.

S'appuyant sur les résultats des études expérimentales un modèle général pour le mécanisme de lixiviation est établi. Les tests courants de lixiviation sont analysés en ce qui concerne leur amélioration par rapport à l'extrapolation des résultats obtenus aux conditions du stockage final posant la base d'expertises de sécurité.

Table of Contents

	<u>Page</u>
1. Introduction	1
2. Performance of Long-Term Leach Tests	4
3. Actinide Leaching Rates for HLW Borosilicate Glasses	7
4. Actinide Leaching Rates for Simulated MLW Cement Products	8
5. Glass/Leachant Interphase Investigations	9
6. Behaviour of Actinides in the Boundary Surface of Glasses	10
7. Chemical Form of Actinides in the Leachant	12
8. General Model for the Leaching Mechanism in Silicate Systems	14
9. Extrapolation of Leach Test Data to Final Disposal Safety Considerations	18
10. Summary and Conclusions	20
Tables	22-28
Figures	29-55
List of Figures	56
References	59

1. Introduction

The immobilization of radioactive wastes in certain qualified products aims at greatest possible durability along any alteration or attack during long final disposal periods to prevent from return of radionuclides into the biosphere also for the maximum credible accident that may happen to the disposal site. In this context main attention is paid to the leaching of radionuclides from final disposal products.

Numerous methods are applied for the determination of leach rates but rather little information is achieved when an assessment for leaching over thousands of years shall be carried out on the basis of these leach test results. For safety evaluations, for public acceptance as well as for geological studies it is obviously necessary to collect more experimental data on the interphase behaviour between solidified waste and leachant, on the mechanism of leaching and on the chemical form of leached isotopes. In this context some fundamental results are reported below to provide some realistic approach to the complex problem and to stimulate discussion on that point.

In a previous publication {1} an evaluation of questions concerning the safety aspects during final disposal is performed on the basis of the relative radiotoxicities of solidified waste products in comparison with naturally occurring 3% uranium ore and its Ra-226 activity respectively. It is implicated that identical quantities of the waste product and uranium ore are completely dissolved in the same volume of leachant, or, that the rate of dissolution is the same for the two compared radioactive solids. But, a more realistic way of thinking shall take into account, that the radiotoxicity of uranium ore does not change over periods of millions of years while the toxicity of the radioactive waste constituents is decreasing along the leaching time because of their relatively short half-lives.

In the Federal Republic of Germany it is considered to solidify the high-level waste arising from the reprocessing of spent LWR fuel in monolithic borosilicate glass cylinders (dimensions: diameter 20 cm, height 80 cm, weight 70 kg), which are placed into underground salt formations for final disposal. Following that strategy the assumptions mentioned below are taken for the subsequent calculations on relative toxicities:

1. A 3% uranium ore of the same weight as the glass bloc is taken as completely "dissolved", starting from the principle that most of the uranium deposits are of secondary genesis by the interaction with water. Thus, uranium mining is generally accomplished on ore bodies near the surface where the ore is penetrated by groundwater since geological periods. There is every reason to believe that the primary high-active glasses will undergo similar metamorphism as the uranium ore if by the greatest credible accident water should contact the glasses.
2. The high level waste glasses are prepared from HLW and base glass just after reprocessing of LWR fuel (burnup 33.000 MWd/metric ton, cooling time: one year, plutonium losses to the waste: 0,3%, uranium losses: 0,1%) and leaching of the glass is starting immediately. The compositions of typical HLW glasses taken for the following calculations are listed in table 1 (columns 2,3). The fission product and actinide compositions are quoted from reference {2}.

The relative radiotoxicities, Tr , are calculated for each isotope following the general equation

$$Tr = O^* \cdot \rho \cdot d \cdot t \cdot (A_O^G \cdot e^{-\lambda t} / A_O^U) \cdot (F^{Ra} / F^i) \cdot 1/G$$

where

- O^* = surface area of the glass block (cm^2), depending on leach rate and time of leaching
- ρ = density of the glass (g/cm^3)
- d = thickness of leached surface layer per year (cm/a)
- t = leaching time in years (a)
- A_O^G = initial specific activity of the considered isotope per gram of glass ($s^{-1}g^{-1}$)
- λ = decay constant for the considered isotope
- A_O^U = specific activity of Ra-226 in 3% uranium ore corresponding to the constant value 10 nCi/g or $370 s^{-1}g^{-1}$, respectively
- F^{Ra} = limit value for the annual ingestion of dissolved Ra-226 activity being $21.5 s^{-1}$ (7)
- F^i = limit value for the annual ingestion of the dissolved activity of the considered isotope (7)
 (Sr-90: $7.2 \cdot 10^2 s^{-1}$, Tc-99: $2.9 \cdot 10^5 s^{-1}$,
 Cs-137: $2.6 \cdot 10^4 s^{-1}$, Pu-239: $7.8 \cdot 10^3 s^{-1}$,
 Am-241: $6.6 \cdot 10^3 s^{-1}$, Np-237: $5.6 \cdot 10^3 s^{-1}$)
- G = total mass of glass block = total mass of uranium ore

The results for the calculated relative toxicities Tr of f.p. isotopes and actinides are expressed by a plot of Tr as a function of the time, t (years), of leaching (see figure 1,2), when a leach rate of $10^{-6} g/cm^2 \cdot d$ is assumed. A compilation of relative toxicities for other leach rates is given in table 2 as well as for infinite leach rates or completely dissolved HLW glass from the beginning.

It is just to put the question on the most probable leach rates or mechanism of leaching when long ranges of time are considered to feed up the hazard evaluation presented above to a realistic assessment.

From the view of their relative radiotoxicities in HLW glasses the only isotopes that have to be taken into consideration with respect to long-term leaching are: Sr-90, Cs-137, Tc-99, Am-241/243, Pu-239/240 and Np-237 (fig.1), whereas the relative toxicities of all other isotopes are by some orders of magnitude lower, thus, their contribution can be neglected.

2. Performance of Long-Term Leach Tests

Specimen Preparation

The specimens to be leached are prepared on laboratory scale. The chemical compositions of the glass samples and the cement samples are listed in table 3.

A larger quantity of glass is prepared by mixing the proper quantity of the base glass frit with the denitrated waste solution. Evaporation of residual water and melting of the glass are performed in a platinum crucible. The prefabricated glass is pulverized, homogenized and molten again in graphite crucibles at 1150°C. From the cylindrical glass samples with 10 mm diameter discs are cut, that are embedded into Araldite, grinded and polished to achieve a well-defined glass surface area in view of the subsequent leach tests.

The cement samples are prepared by mixing an appropriate amount of cement with the plutonium/americiu-nitrate solution neutralized by the addition of sodium hydroxide solution. This pasty homogenized mixture is pressed into Teflon tubes. After the cement has set the samples are removed from the tubes and introduced into a wet atmosphere for hardening of the cement. The samples are ready for use after 30 days. Well-shaped cylindrical specimens are cut from the larger samples for the performance of the subsequent leach tests.

In figure 3-10 a series of α -autoradiographs is shown to demonstrate the homogeneity of the samples before leaching.

The dimensions for the specimens are taken such that the surface area exposed to the leachant does not change by more than 5% over the whole leaching time.

Specimen/Leachant Container

The specimen is suspended on a platinum wire, that is fixed to the cap of the leachant container being constructed of polyethylen.

The volume of the leachant is taken such that the value of the ratio $\frac{\text{volume of leachant}}{\text{exposed surface area of specimen}}$ is 10 cm. When the proper volume is introduced into the leachant container it is closed by the cap with the hanging down specimen assuring that the specimens surface is completely covered by the leachant from all sides. The leach test is performed at a temperature of $23 \pm 1^\circ\text{C}$. (composition (wt.%) of carnallite solution: 62.83 H_2O ; 2.04 MgSO_4 ; 34.3 MgCl_2 ; 0.62 KCl ; 0.21 NaCl), corresponds to an equilibrium solution from water leached natural rock salt deposits.

Sampling of Leachant

After certain intervals (see figures 11-15), depending rather on the sensitivity of analytical instruments for radionuclide determination in the leachant, the cap with the hanging down specimen is withdrawn from the first leachant container and immediately brought to a second one filled with fresh leachant, an so on.

The first and all further leachant containers are carefully closed, containing all leached material from the test specimen taking into account all dissolved as well as suspended or adsorbed substances for the following analytical determinations, carried out on the whole leachant sample enclosed in the container.

Analytical Determinations

All analytical determinations for leached radioisotopes are performed by γ -spectrometric and γ -counting techniques with the exception of measurements in demineralized water leachants, that may be carried out with α -spectrometric methods. But, to assure that the small sample taken for α -counting is representative for the whole leachant other isotopes with similar chemical behaviour as that measured only by α -spectrometry shall be determined by both α - and γ -spectrometric methods - if necessary to get any correction factor for the results from α -counting. The latter method is applied for the determination of Cm-242 (α , no γ) and Am-241 (α , 60 keV γ), see figure 15.

For calibration of the γ -spectrometric equipment the pure leaching solutions are doped with known proper amounts of the isotopes to be measured. The volume of leachant and the dimensions of the container are the same as used for the leach tests.

Plutonium of mixed isotopic composition is determined by the 150 keV γ -line of the Pu-241 isotope, americium by its 60 keV γ -line.

From the results of the γ -spectrometric measurements the incremental leaching rates, R , are calculated and plotted as a function of the time of leaching, t , where

$$R = \frac{a_n}{A_0 \cdot F \cdot t_n}$$

R = incremental leaching rate ($\text{g} \cdot \text{cm}^{-2} \cdot \text{day}^{-1}$)

a_n = radioactivity (s^{-1}) leached during each leaching period, t_n .

A_0 = specific radioactivity ($\text{s}^{-1} \cdot \text{g}^{-1}$) initially present in the specimen

F = exposed surface area of the specimen (cm^2)

t_n = duration of each leaching period (days)

t = cumulative leaching time

3. Actinide Leaching Rates for HLW Borosilicate Glasses

The graphs for the leaching rates of plutonium and americium from highly actinide doped HLW borosilicate glass specimens (compositions see table 3) leached by various solutions are shown in figure 13-15.

The zigzag variations of the leaching rates with the time are not attributed to any inaccuracy due to the analytical procedure. The effect is rather explained by the non-uniform leaching which is demonstrated by the appearance of the leached glass surface (see paragraph 5) and will be discussed later in paragraph 8.

The leach rates for americium (fig.15) in various dilute aqueous solutions are not very different from one another, they are in the range of $(0.5 \dots 5) \cdot 10^{-6} \text{ g/cm}^2 \cdot \text{d}$, while the leach rates in saturated carnallite solutions are in the range of $(0.3 \dots 3) \cdot 10^{-5} \text{ g/cm}^2 \cdot \text{d}$.

As for the plutonium specimens, rather high plutonium concentrations are molten into the glass in view of the poor sensitivity of the measuring device for plutonium determination in the leachant. The specimens containing 2 wt.% plutonium-oxide are completely homogeneous whereas the specimens containing 10 wt.% plutonium-oxide are composed of a plutonium saturated glass matrix and a crystalline oxide phase highly enriched of plutonium oxide.

Independent on the kind of the leaching solution the leaching rates for plutonium from the 2 wt.% glasses (fig. 13) are in the range of $(2 \dots 3) \cdot 10^{-7} \text{ g/cm}^2 \cdot \text{d}$, and from the 10 wt.% glasses (fig. 14) the leaching rates for plutonium are in the range of $(1 \dots 6) \cdot 10^{-7} \text{ g/cm}^2 \cdot \text{d}$. There is no significant difference between the single phase and the second phase glass products.

A prolongation of the long-term leach tests may be considered, but as demonstrated for the americium lixiviation by demineralized water (fig. 15), the leach rate becomes virtually constant after about one month and no benefit derives from the eight months test.

4. Actinide Leaching Rates for Simulated MLW Cement Products +)

On the cement products listed in table 3 the leaching rates of plutonium and americium are measured and the graphs plotted in figures 11, 12.

It is striking that the leach rates of americium and plutonium are of the same order of magnitude and are at the same time independent on the sodium nitrate content of the cement products.

For dilute aqueous leachants the leach rates are in the range of $(2 \dots 11) \cdot 10^{-7} \text{ g/cm}^2 \cdot \text{d}$. In saturated carnallite solutions the leach rates are decreasing to values lower than $5 \cdot 10^{-5} \text{ g/cm}^2 \cdot \text{d}$. Obviously the leaching time has to be extended for leach tests in saturated salt solutions.

It has to be noticed that the leach rates of the actinides are in general somewhat lower for the cement products as for the glass products.

+) idealized products, in which the medium level waste is only represented by sodium nitrate and actinides

5. Glass/Leachant Interphase Investigations

After being leached the surface of the glass specimen is observed with the scanning electron microscope. Prior to observation the freshly leached glass is cleaned with demineralized water and subsequently carefully dried at $23 \pm 1^\circ\text{C}$ in wet and later on in dry atmosphere for more than three days.

The appearance of the surface of the different glass specimens leached by different leaching media is just as strikingly different, looking at figures 16-24. It shall be mentioned that the pictures taken are in any case reproducible.

It seems audacious to bring forth an explanation for these significant differences. But, obviously there are layers of the silicate matter which are withdrawn from the glass matrix as more or less small particles. Blasting of the surface layer may be accounted for the swelling of the vitreous silicate structure due to the attack of water that is chemically introduced into the polymer silicate system. And undoubtedly it takes some time of leaching until the surface layer bursts and the leachant will get access to the fresh virginal glass below.

Kind and velocity of surface attack and cracking is dependent on the leaching temperature and on the nature of the leachant. Obviously the mechanism seems different for dilute aqueous leachants and for concentrated salt solutions as shown for the attack of saturated carnallite solution in figures 18, 21, 24, although the leaching rates for plutonium and americium are not significantly different. It is therefore, that either much more smaller particles are withdrawn from the glass surface with increasing salt concentrations in the leachant or the attack of water molecules and its ions is forced back by ion exchange mechanisms comprising the saline components in the leaching solution. As for carnallite solutions, it is known from common literature that magnesium ions are replacing alkali and earth alkali ions combined to silicate structures like those occurring in cement or concrete.

6. Behaviour of Actinides in the Boundary Surface of Glasses

The working basis for the evaluation of the behaviour of actinides in the boundary surface of leached glass is established by measurement of the energy loss of α -particles in the solid matter. A standardization of the energy loss values and of the shape of energy spectra of HLW glasses with homogeneous distributions of the actinides is performed on the different types of glasses {3}.

The leached specimens being measured have a total plutonium content of 2.0 wt.% PuO_2 . The ratio of the α -activities of Pu-238 and Pu-239 is 1.85:1, whereas the α -activity of Am-241 contributes only with 8% to the Pu-238 activity peak. Thus, for the evaluation of the separate Pu-238 and Pu-239 peaks the contribution of Am-241 is neglected.

Corresponding to the measured energy loss values for the non-leached specimens {3} the stopping powers dE/dx ($\text{MeV}/\text{mg}\cdot\text{cm}^{-2}$) are calculated and converted to the relation between the thickness of the absorbing layer and the remaining α -particle energy for the different decay energies for Pu-238 ($E_\alpha = 5.50$ MeV) and Pu-239 ($E_\alpha = 5.15$ MeV). On the basis of these results the measured values on the leached specimens are converted and the graphs plotted as a function of the PuO_2 -concentration versus α -energy (channel number), figure 25.

From figure 25 the total plutonium concentrations are calculated from the peak areas measured at the surface of the leached specimens. The ratio of the areas for both peaks showing plutonium enrichment in the surface layer shall be 1.85:1 for the Pu-238 and Pu-239 peaks according to the activity levels in the glass matrix mentioned above. The values measured (figure 25) are in the range of 1.6:1.

All the peaks are showing increasing partial areas with increasing energies, which points out that plutonium enrichment is highest at the contact surface glass/leachant and decreases rapidly in the surface layer until the plutonium concentration of the glass is reached.

In table 4 the approximate values for the average thickness of surface layers and the average plutonium concentrations are listed. The thickness of the layer is in the order of $1\mu\text{m}$ and it decreases slightly with decreasing alkali content of the glass. A similar trend is indicated by the drop of plutonium enrichment. For HLW glasses leached with saturated carnallite solutions no plutonium enrichment can be detected.

From the preceding experimental results it can be concluded:

1. The maximum average thickness of the surface layer that adheres to HLW borosilicate glass after being leached by dilute aqueous solutions is in the order of $1\mu\text{m}$.
2. The apparent plutonium enrichment in the surface layer can be accounted for the virtually rapid lixiviation of sodium ions from the glass with respect to plutonium lixiviation. The measured increase of the plutonium concentration corresponds to the feasible release of sodium as well as no plutonium enrichment occurs in saturated salt (carnallite) solutions where sodium lixiviation is either suppressed or where sodium is exchanged for other metal cations like magnesium ions.
3. Very probably the plutonium goes with the remaining silicate system or still bonded to silicate polymers into the leaching solution.

7. Chemical Form of Actinides in the Leachant

From the portrait of the experimental results described so far it can be supposed that the actinides apparently dissolved in the leachant are still bonded may be chemically or physically to silicate polymers in the leaching solutions, too.

It is of predominant interest to get knowledge about the properties of those actinides dissolved in leaching media as a basis for the evaluation of pathways of the actinides in geologic formations or soils. In this context an attempt at the experimental determination of the molecular size of actinides leached from HLW borosilicate glass products by demineralized water has been made.

Two independent methods have been applied for particle size measurements:

1. Filtration of the leachants over molecular filters, membrane Pellicon Type PTGC, with nominal permeability for organic macromolecules of molecular weights up to 10 000 which are corresponding to spheric particles sizes of 32 Å.
2. Light scattering measurements on the leachants with a Brice-Phoenix light scattering photometer model 2000 and a Brice-Phoenix differential refractometer model BP-2000-V, using unpolarized light with a wavelength of 546 mμ.

Experimental:

Two glass specimens No.A 2/5 and No.P 2/2 (composition see table 3) are leached with demineralized water at 23 ± 1 C°. At the end of the leach test (100 days) the leachants are analyzed on the particle size of leached material by the two procedures mentioned above.

Procedure 1:

The activities of the apparently clear solutions (leachants) are determined by alpha-spectrometric and alpha-counting techniques as well as the activities of the solutions that are obtained after filtering the original solutions over Pellicon Type filters.

The results are shown in table 5.

Procedure 2:

Light scattering measurements were made on the leaching solutions using a Brice-Phoenix light scattering photometer {5}. The increase in refraction index (Δn), due to dissolved material was measured with a Brice-Phoenix differential refractometer {4}. The value of Δn is needed to estimate the average molecular weight of particles. The turbidity is calculated following the procedure explained in operational manual OM 2000 for the Brice-Phoenix light scattering photometer and the theory from reference {5}. Similar measurements on solutions of Ce^{4+} in $HClO_4$ are reported in reference {6} in more detail deviating only by a filtration step preceding the measurement.

The turbidity, τ , the refractive index, Δn ($\Delta n = n - n_0$, n : refractive index of the solution, n_0 : refractive index of the solvent - water-), and the concentration of dissolved material is presented in table 6.

As the actinide content of the solutions is too low to contribute considerably to the scattering polymer silicate molecules are taken for molecular weight calculations.

Molecular weights can be estimated using the equation $Hc/\tau = 1/M + 2 Bc$. The molecular weight M is determined by measuring and calculating Hc/τ for various dilute solution with $H = 6.18 \cdot 10^{-5} n^2 \left(\frac{\Delta n}{c} \right)^2$. Following these procedures, the molecular weights shown in table 7 are estimated as well as the corresponding particle sizes calculated from silicate lattice parameters.

Interpretation of Results:

From the results listed in table 5 it is demonstrated, that all the actinides are predominantly bonded to high molecular particles with a diameter exceeding $0.32 \cdot 10^{-2} \mu\text{m}$. The average particle size determined by light scattering measurements is in the range of $10^{-2} \mu\text{m}$ (see table 7). As the actinide content of the solutions is too low to contribute considerably to the scattering it is evident that the actinides are tightly fixed to silicate polymers occurring in the leaching solutions.

8. General Model for the Leaching Mechanism in Silicate Systems

The performance of a general model for the leaching mechanism from glass and other silicate systems shall be based on the results of the investigations, reported above, the main topics are summarized as follows:

1. Generally, the order of magnitude of the leach rates for actinides is 10^{-6} g/cm² · d for borosilicate glass products leached with dilute aqueous solutions, and 10^{-5} g/cm² · d when leached with saturated carnallite solution.

The leach rates for actinides leached from cement products are slightly lower compared to the glass products, except those values obtained for saturated carnallite solutions, which are higher for cement products.

2. The interphase of the glass exposed to the leachant is attacked by water and its ions to form siliceous gels, when the leachant is pure water or a diluted salt solution. Otherwise, at high salt concentrations in the leachant the corresponding metal ions are involved in the corrosion process occurring to the virgin silicate products.

3. The surface layer affected by water is swelling, and when the swollen layer has arrived at a certain thickness in the range of 1 μm it bursts open and is subsequently withdrawn from the glass into the leachant.

When saturated salt solutions are involved in the leaching process, no swelling is observed.

4. The particles that are actually dissolved from the glass by water are composed of high polymer siliceous matter with an average particle size of 10^{-2} μm.
5. The actinides are still bonded to the silicate polymers within the leaching solution.

Now, with respect to the experimental results briefly listed above, the following conclusions are verified:

Silicate systems like glasses build up a swelling boundary surface when attacked by water or dilute aqueous solutions in the course of which the virginal silicate matter is screened against lixiviation up to a certain thickness of the adhering layer. When the layer bursts the attack starts or increases again on the unaffected matter. Thus, the leaching mechanism is characterized by successive periods of decreasing and increasing lixiviation. The sequences are not uniform in their extension and amplitude with time, as indicated by the graphs of the leaching rates versus time and by the inhomogeneous detachment of swollen particles from the surface, respectively.

But, nevertheless the average leach rate remains constant when being measured over a long range of time.

As a consequence of that leaching mechanism the leach rates of all components of the silicate system, in particular for homogeneous systems like glass, are expected to be identical. It is shown by the graphs of the leach rates for americium and plutonium that the leachability of plutonium is lower by a factor of 2 to 6. These deviating results may be attributed to experimental errors but the more to the fact that competitive ion exchange or adsorption reactions are taking place: these effects can be neglected when the leaching time is considerably extended. That means, the 80 or 240 days tests reported in paragraph 3 are corresponding to an average thickness of the leached glass surface of only 0.3 to 1 μm , approximately equal to the mean one-layer-lixiviation. If better statistics are desired the leach tests have therefore to be extended to several years. In support of the proposed leaching mechanism long-term leach tests are started for the determination of the leaching rates of alkali ions. Up till now the results indicate that the leach rates are decreasing with time apparently sloping to values in the range of those measured for the actinides.

Unless there are still some questions on the mechanism it has to be pointed out that the measured leach rates are in any case the highest or most conservative one's in view of the fact that the mentioned ion exchange and adsorption effects interfering at short-term leach tests (~100 days) are producing increased leach rates for ions with more ionic character, higher mobility and greater solubility as is to be expected for the values of the leach rates from long-term tests (years) according to the overall mechanism.

At high ionic concentrations in the leaching solution as in the case of saturated carnallite solution ion exchange processes and cation induced break of linkages in the primary polymer silicate systems may be considered as the main driving forces for the lixiviation. From the available data it is impossible to make an attempt on the description of the mechanism. But it seems to be reasonable to hold the following subjects in mind:

1. The leach rates of the actinides from glass as well as from cement products are significantly higher in the beginning of the leach test. The shape of the curves, leach rate versus time, is quite different from that obtained for dilute aqueous solutions: there is no more the typical zigzag line but a rather straight sloping line that leads to decreasing values of the leach rates at increasing leaching times.
2. The leached surface layer of the glass specimens looks quite unaffected in spite of the fact that a considerable amount of material is leached. This curious behaviour may be explained either by an integrated ion exchange process taking place without any significant geometrical alteration of the compact glass system or by a homogeneous separation of very small particles from the whole surface area or by a combined advance of both mechanisms.

The fact that the concentration of actinides in the boundary surface does not change during leaching supports for the second or the combined mechanism.

Finally, it can be supposed that the leaching mechanism studied on borosilicate glasses is to be applied to other silicate systems which are microscopically homogeneous. Similar considerations may be suitable for the evaluation of cement products.

In figure 26 and 27 the appearance of a cement product observed with the scanning electron microscope before and after leaching is shown. Upon leaching the relatively dense product turns to a microporous matter accounting for the low leach rates of the actinides in comparison to the leach rates of actinides immobilized in glass: Obviously, the formed macromolecular siliceous particles containing the actinides are retained to some extent within the remaining porous system.

9. Extrapolation of Leach Test Data to Final Disposal Safety Considerations

As the greatest credible accident which may occur to the final disposal site the intrusion of water is considered followed by the lixiviation of the immobilized radioactive waste products. From the considerations outlined in paragraph 1 the most conservative advance to the calculation of leached radioisotopes over long periods of time and of their relative radio-toxicities compared to 3% uranium ore will be performed on the real solidification products when leaching starts with deposition.

In this sense the extrapolation of leach test results has to be done taking into account the following marginal conditions:

1. Evaluation of the temperature/time curve for the water-penetrated disposal site.
2. Chemical composition of the penetrating aqueous solution
3. Measurement of the long-term leach rates according to paragraph 2 with regard to item 1 and 2 (temperature and composition of leachant)
4. Dimensions of solidified waste products

With respect to the experimental results which have shown that more or less extended flakes are detached from the siliceous solidification products by the attack of dilute aqueous solutions in the run of relatively short-term leach tests (~100 days, ambient temperature), it can be assumed that over long periods of time a quasi homogeneous leaching of the solid matter takes place as the average of successive layer detachments.

The determination of leach rates has to be performed on larger samples (conditions see paragraph 2) with regard to the mechanism of leaching (paragraph 8). The smallest specimen diameter shall be at least 100 times the average thickness of the leached surface layer(s) or more for the whole leaching time. According to a 100 days leach test with $R = 10^{-6} \text{ g/cm}^2 \cdot \text{d}$ the specimen diameter shall be greater than 0.1 mm, it shall be greater than 10 mm for $R = 10^{-4} \text{ g/cm}^2 \cdot \text{d}$. If the specimens are smaller they probably will burst due to their swelling.

Therefore, the results of leach tests performed on granules or very small specimens - above all at higher temperatures or higher leach rates as in the case of soxhlet tests - are not suitable for any extrapolation to long-range lixiviation. The question raises, to what extent these tests are applicable to the intercomparison of products, in the light of the leaching mechanism and its consequences mentioned above.

10. Summary and Conclusions

A series of results from investigations on the leaching behaviour of actinides from HLW borosilicate glasses and MLW cement products is presented comprising the determination of leaching rates in various aqueous solutions, the measurement of actinides in the boundary surface of leached glass specimens, the microscopic demonstration of leached surface layers and an estimation on the chemical form of actinides in aqueous leachants.

On the basis of the experimental results an evaluation of the processes which take place during the leaching of silicate systems is performed and an appropriate leaching mechanism is established, including a critical review of different leach test procedures and a proposal for the performance of long-term leach tests with regard to their extrapolation to final disposal requirements.

Although something has come to light it shall be noticed that there are several questions still open concerning the lixiviation at higher temperatures, the leaching with saturated salt solutions and the chemical form and behaviour of actinides, Np-237 especially, in leachants with high salt concentrations.

Acknowledgement:

We would like to thank for experimental help and performance of the numerous analytical determinations:

H. Kreiselmeier

Abteilung Strahlenschutz und Sicherheit

D. Hentschel

Abteilung Behandlung Radioaktiver Abfälle

component	Average Composition (wt.-%)		
	base glass	HLW glass	HLW glass + Gd ₂ O ₃ poison
base glass:			
SiO ₂	50.5	40.2	35.1
TiO ₂	4.2	3.3	2.9
Al ₂ O ₃	1.4	1.1	1.0
B ₂ O ₃	13.6	10.8	9.5
CaO	2.8	2.2	2.0
Na ₂ O	27.5	21.9	19.1
fissionproducts		16.68	16.68
actinides		1.06	1.06
corrosion products		2.69	2.69
Gd ₂ O ₃ poisoning			10.0

fission products (wt.-%)			
SeO ₂	0.034	Rb ₂ O	0.175
SrO	0.498	Y ₂ O ₃	0.282
(⁹⁰ SrO)	(0.300)	ZrO ₂	2.360
MoO ₃	2.470	⁹⁹ TcO ₂	0.526
Ru	1.060	Rh	0.187
(¹⁰⁶ Ru)	(0.039)	Pd	0.635
Ag	0.028	CdO	0.045
SnO	0.031	Sb ₂ O ₃	0.010
TeO ₂	0.346	BaO	0.760
Cs ₂ O	1.360	La ₂ O ₃	0.710
(¹³⁷ Cs ₂ O)	(0.610)	Nd ₂ O ₃	2.230
Ce ₂ O ₃	1.600	Pr ₂ O ₃	0.670
(¹⁴⁴ Ce ₂ O ₃)	(0.080)	Pm ₂ O ₃	0.051
Sm ₂ O ₃	0.455	Eu ₂ O ₃	0.099
(¹⁵¹ Sm ₂ O ₃)	(0.023)	(¹⁵⁴ Eu ₂ O ₃)	(0.025)
Gd ₂ O ₃	0.056	(¹⁵⁵ Eu ₂ O ₃)	(0.002)

actinides (wt.-%)	
UO ₂	0.516
²³⁷ NpO ₂	0.412
²⁴¹ AmO ₂	0.050
²⁴³ AmO ₂	0.0476
²⁴² CmO ₂	0.0010
²⁴⁴ CmO ₂	0.0162
²³⁸ PuO ₂	0.0003
²³⁹ PuO ₂	0.0087
²⁴⁰ PuO ₂	0.0035
²⁴¹ PuO ₂	0.0016
²⁴² PuO ₂	0.0006
corrosion products (wt.-%)	
Fe ₂ O ₃	1.870
Cr ₂ O ₃	0.530
NiO	0.290

Table 1: Composition of LWR high-level waste glass products

leach rate (g/cm ² ·d)	isotope	leaching time (years)					
		10	10 ²	10 ³	10 ⁴	10 ⁵	10 ⁶
∞	Sr-90	8.4 · 10 ⁵	9.4 · 10 ⁴	-	-	-	-
	Cs-137	3.2 · 10 ⁴	4.0 · 10 ³	-	-	-	-
	Tc-99	0.5	0.5	0.5	0.5	0.36	0.014
	Am-241	29.0	25.0	5.9	-	-	-
	Am-243	25.0	25.0	25.0	9.4	0.002	-
	Pu-240	4.6	10.0	9.5	3.7	-	-
	Pu-239	1.3	1.3	1.9	4.7	0.68	-
	Np-237	0.95	0.95	0.95	0.95	0.95	0.69
10 ⁻⁴	Sr-90	2.5 · 10 ⁴	2.8 · 10 ⁴	-	-	-	-
	Cs-137	9.5 · 10 ²	1.1 · 10 ³	-	-	-	-
	Tc-99	0.007	0.07	0.5	0.5	0.36	0.014
	Am-241	0.41	3.6	5.3	-	-	-
	Am-243	0.7	7.0	24.0	9.3	0.002	-
	Pu-240	0.065	1.5	8.5	3.6	-	-
	Pu-239	0.018	0.18	1.7	4.7	0.68	-
	Np-237	0.013	0.13	0.86	0.95	0.95	0.69
10 ⁻⁶	Sr-90	2.5 · 10 ²	2.8 · 10 ²	-	-	-	-
	Cs-137	9.5	11.0	-	-	-	-
	Tc-99	-	-	0.007	0.07	0.36	0.014
	Am-241	0.005	0.004	0.083	-	-	-
	Am-243	0.007	0.07	0.35	1.4	0.002	-
	Pu-240	-	0.015	0.14	0.52	-	-
	Pu-239	-	0.002	0.027	0.67	0.68	-
	Np-237	-	0.001	0.013	0.13	0.86	0.69
10 ⁻⁸	Sr-90	2.5	2.8	-	-	-	-
	Cs-137	0.095	0.11	-	-	-	-
	Tc-99	-	-	-	-	0.004	-
	Am-241	-	-	-	-	-	-
	Am-243	-	-	0.004	0.014	-	-
	Pu-240	-	-	0.001	0.005	-	-
	Pu-239	-	-	-	0.007	0.007	-
	Np-237	-	-	-	0.001	0.013	0.098

Table 2: Calculated relative radiotoxicities, $Tr \cong 10^{-3}$, of significant isotopes leached from HLW glass blocks with different leach rates

N ^o of specimen	composition of glass specimens (wt.-%)					
	base glass ¹⁾	f.p. oxides ²⁾ + c.p. oxides	Gd ₂ O ₃	AmO ₂	PuO ₂	CmO ₂
A 1/5	95.07	-	-	4.90	-	0.03
A 2/5	78.43	16.64	-	4.90	-	0.03
A 3/5	68.93	16.65	9.51	4.88	-	0.03
P 1/2	98.00	-	-	0.005	2.00	-
P 2/2	80.85	17.15	-	0.005	2.00	-
P 3/2	71.05	17.15	9.80	0.005	2.00	-
P 1/10	90.00	-	-	0.025	9.98	-
P 2/10	74.25	15.75	-	0.025	9.98	-
P 3/10	65.25	15.75	9.00	0.025	9.98	-

(1) composition of base glass, see table 1.

(2) composition of fission product oxides and corrosion product oxides, see table 1 (f.p. oxides replaced by the corresponding inactive isotopes, Tc replaced by Mn)

N ^o of specimen	composition of cement specimens (wt.-%)				
	cement ³⁾	NaNO ₃	PuO ₂	AmO ₂	H ₂ O
C 1	75.7	8.56	0.86	0.002	14.9
C 2	81.2	1.08	0.86	0.002	16.9
C 3	75.9	5.92	3.44	0.008	14.7
C 4	76.8	4.30	3.44	0.008	15.5

(3) composition of cement (wt.-%): 62 CaO, 23 SiO₂, 7 Al₂O₃+TiO₂, 4.5 Fe₂O₃, 2.0 MgO, 1.5 SO₃

Table 3: Chemical composition of glass and cement specimens used for the leach tests

measuring results		N ⁰ of leached glass specimen ¹⁾		
		P 1/2	P 2/2	P 3/2
dE/dx (keV/ μ m) ²⁾	Pu-238	144	166	176
	Pu-239	151	174	184
average thickness of the surface layer (μ m)	<u>leachant:</u> demineralized water	1.2	1.0	0.4
	1 M NaCl-solution	1.7/2.3 ³⁾	1.2	1.1
	saturated carnalite solution	0.8	-	-
average PuO ₂ -concentration in the surface layer (%)	demineralized water	4	2.3	2.3
	1 M NaCl-solution	5	2.3	2.3
	saturated carnalite solution	2.2	-	-

- (1) Composition of glasses N⁰ P 1/2, P 2/2, P 3/2, see table 3.
- (2) According to the low value for the thickness of the surface layer, dE/dx is assumed to be constant. One channel in the alpha-spectrum corresponds to 0.05 μ m.
- (3) The values are corresponding to the thickness of two layers (figure 25); the outward layer has detached from the inner layer by about 2 μ m.

Table 4: Results from the measurement of the energy loss of alpha-particles escaping from the surface of leached glass specimens

activity of leaching solution and DF		isotope in the leaching solution		
specimen N ^o		Cm-242	Am-241	Pu _{tot.}
A 2/5 ¹⁾	original (s ⁻¹ .ml ⁻¹)	1.92 · 10 ⁴	1.41 · 10 ⁴	-
	after filtration (s ⁻¹ .ml ⁻¹)	1.00	1.26 · 10 ²	-
	DF(2)	1.92 · 10 ⁴	1.12 · 10 ²	-
P 2/2 ¹⁾	original (s ⁻¹ .ml ⁻¹)	-	2.04 · 10 ⁴	3.33 · 10 ⁴
	after filtration (s ⁻¹ .ml ⁻¹)	-	8.15	3.37 · 10 ³
	DF(2)	-	2.50 · 10 ³	9.90

(1) Composition of specimens N^o A 2/5 and P 2/2, see table 3.

(2) The DF values shall be considered in a qualified sense with respect to the filtering technique. The obtained values are dependent on the geometrical shape and the total mass of the filtered particles.

Table 5: Activity of leaching solutions before and after filtering over Pellicon Type filters (0.32 · 10⁻² μm)

measurement values	leaching solution from specimen N ^o		
	base glass ¹⁾	A 2/5 ²⁾	P 2/2 ²⁾
$\tau \cdot 10^4$	6.218	76.62	35.12
$\Delta n \cdot 10^5$	4.87	7.70	10.2
$c \text{ (g/ml)} \cdot 10^3$	0.20	0.40	0.55

(1) Composition, see table 1.

(2) Composition, see table 3.

Table 6: Turbidity, refractive index increment and concentration of the leaching solutions

calculated values ¹⁾	leaching solution from specimen N ^o		
	base glass ²⁾	A 2/5 ³⁾	P 2/2 ³⁾
average molecular weight (\bar{M})	$0.5 \cdot 10^6$	$4.7 \cdot 10^6$	$1.7 \cdot 10^6$
average particle size (μm)	$0.96 \cdot 10^{-2}$	$2.00 \cdot 10^{-2}$	$1.43 \cdot 10^{-2}$
main radioactive isotope	-	Am, Cm	Pu, Am

(1) The values are calculated from the values measured and listed in table 6, lattice parameters and molecular compositions of the glass specimens.

(2) Composition, see table 1.

(3) Composition, see table 3.

Table 7: Molecular weight and particle size of silicate polymers in aqueous leachants from borosilicate glasses

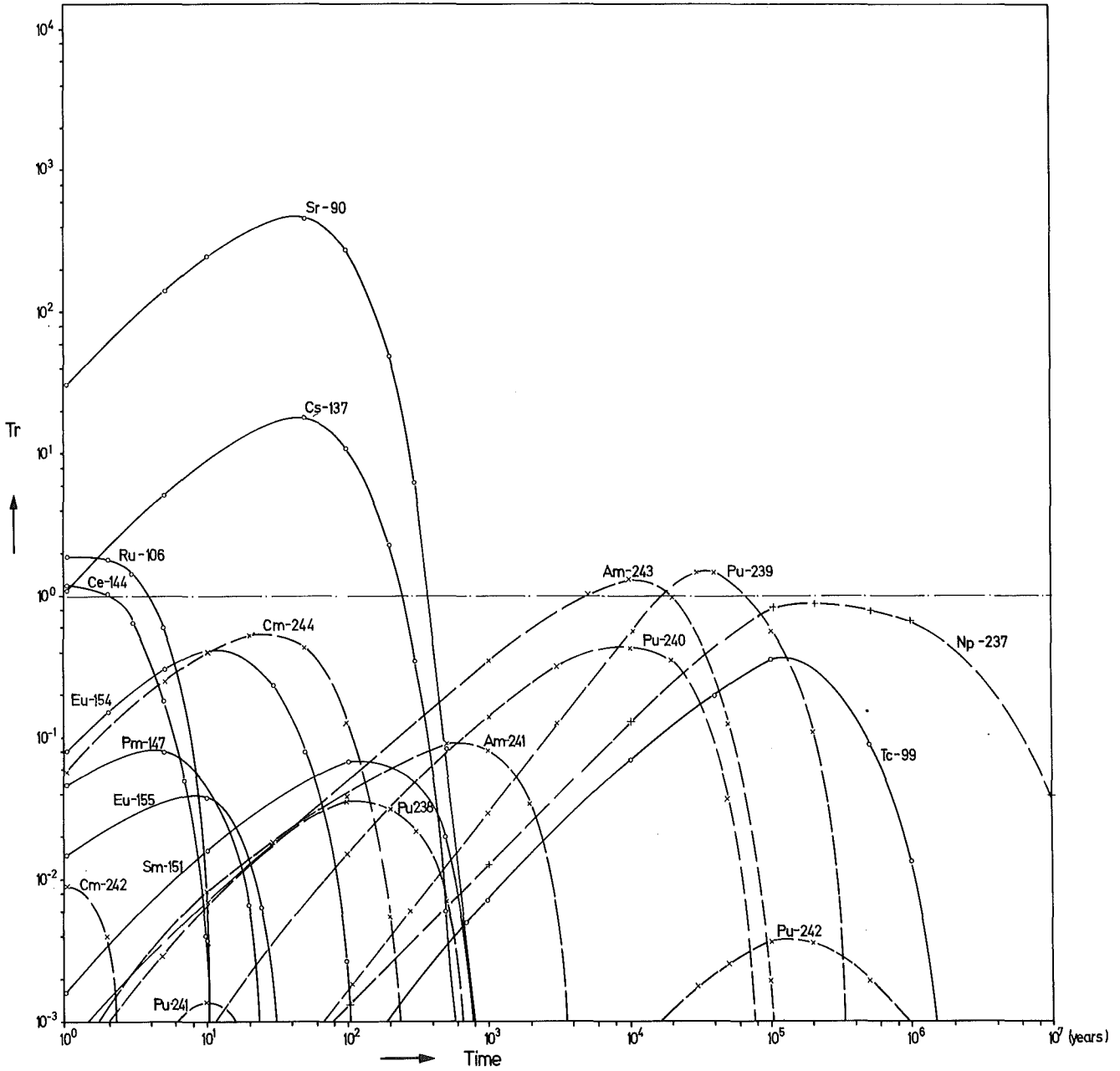
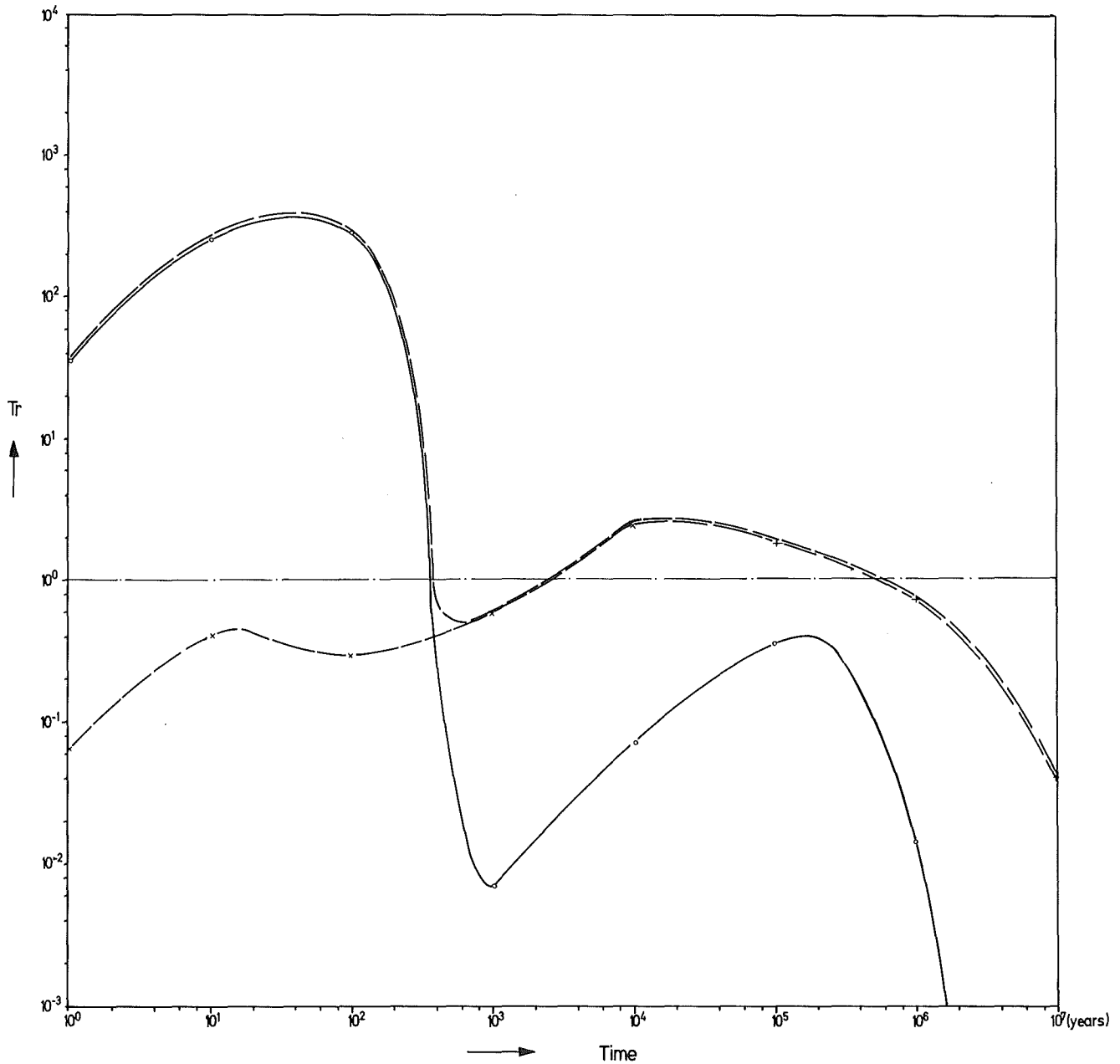
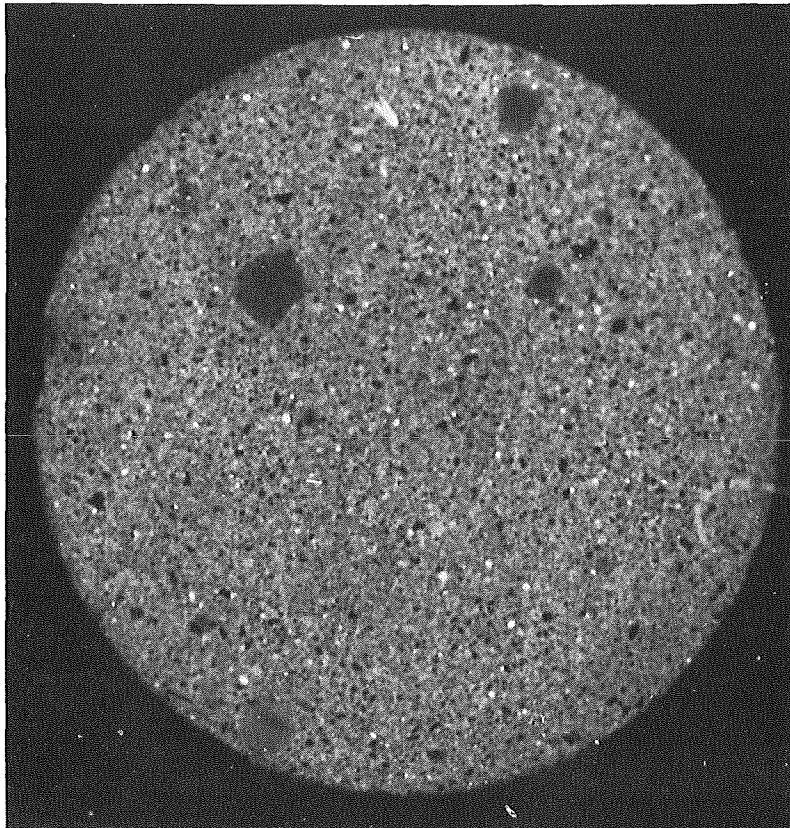


Figure 1: Calculated relative radiotoxicities of fission products and actinides leached from monolithic HLW glass blocks (leach rate $R = 10^{-6} \text{ g/cm}^2 \cdot \text{d}$)

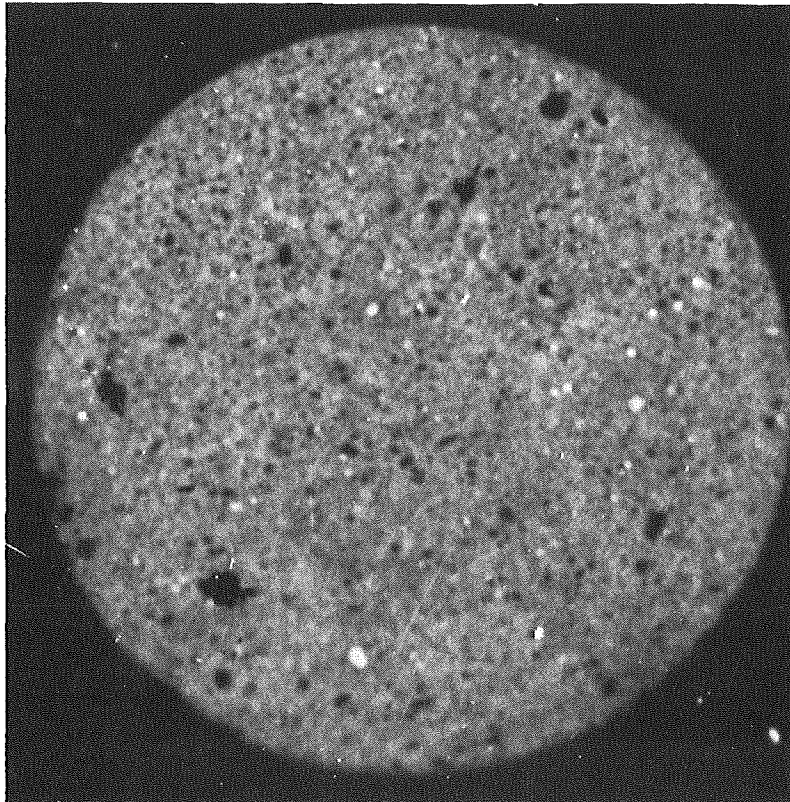


— fission products; -x-x- actinides;
--- total

Figure 2: Calculated relative radiotoxicities for the total of fission products and actinides leached from monolithic HLW glass blocks (leach rate $R = 10^{-6} \text{ g/cm}^2 \cdot \text{d}$)

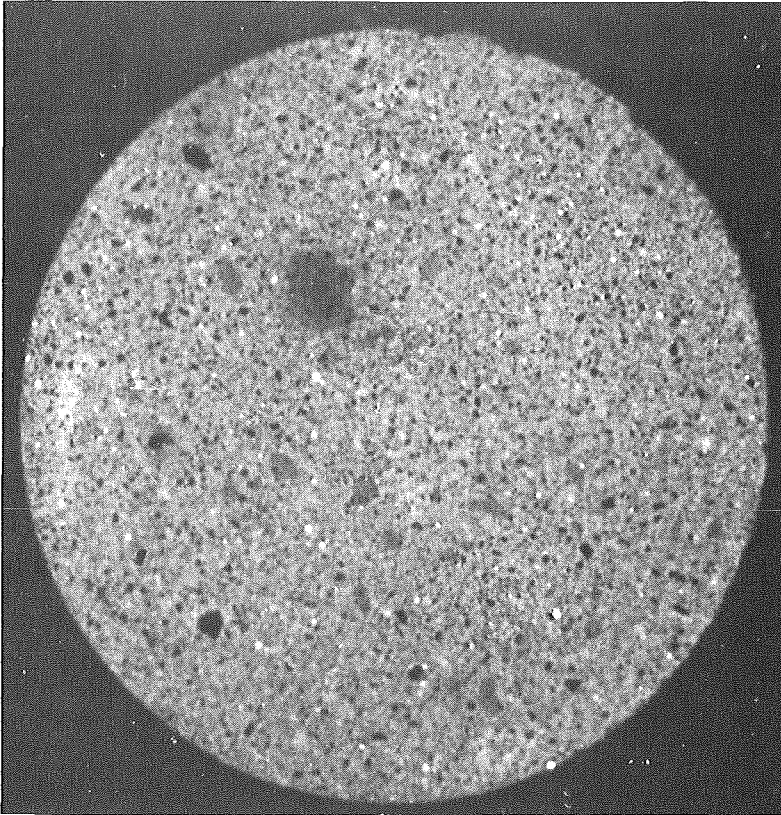


specimen
No C1

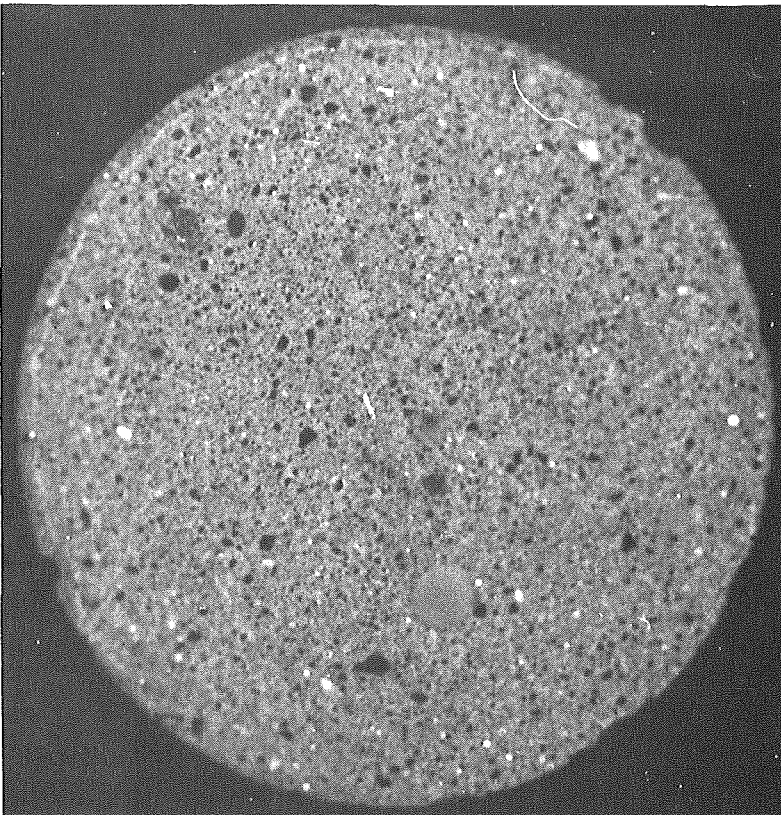


specimen
No C2

Figure 3: Alpha autoradiographs of cement specimens used for leach tests

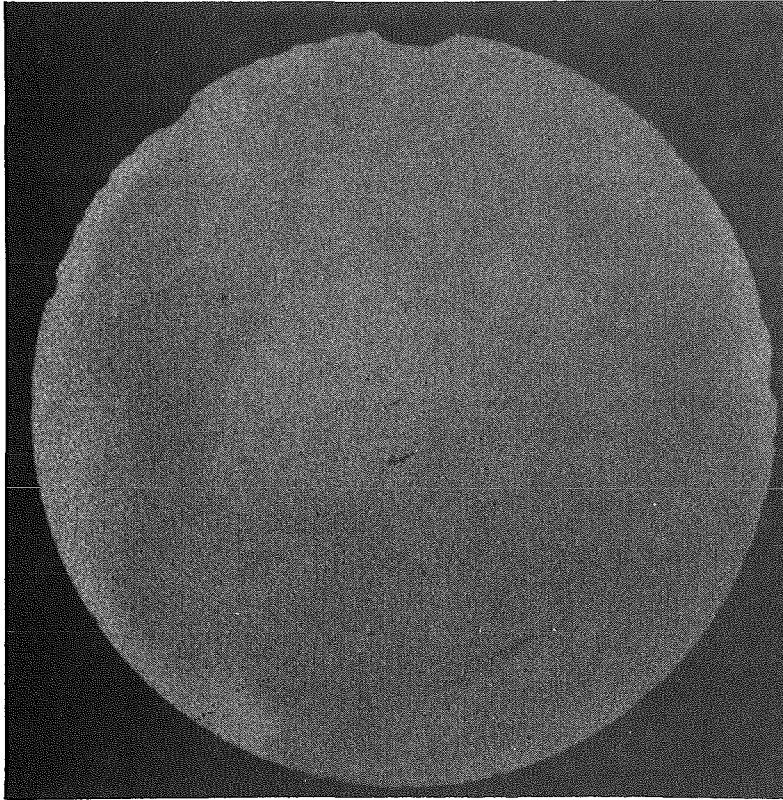


specimen
No C3

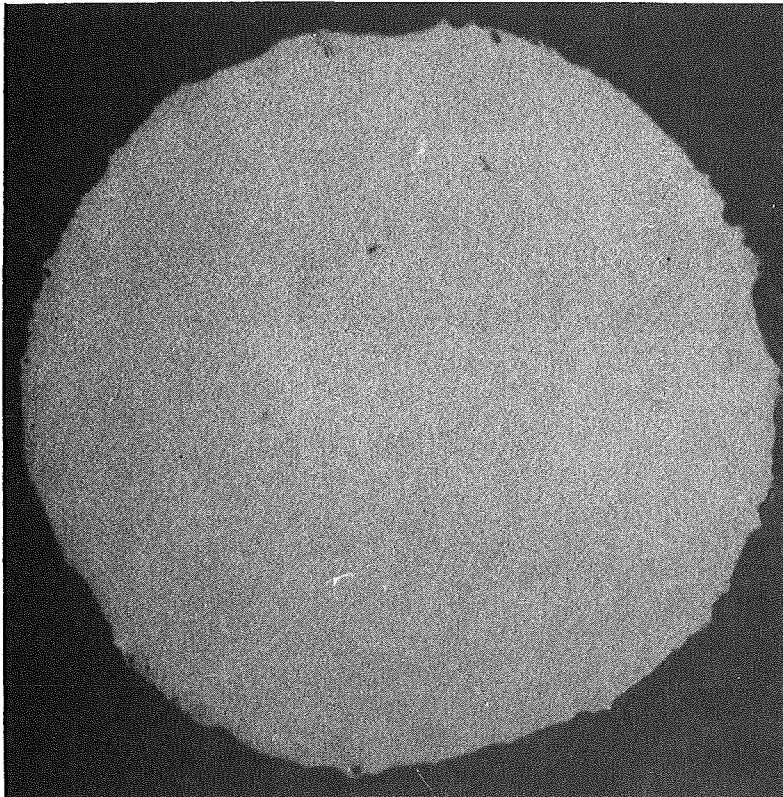


specimen
No C4

Figure 4: Alpha autoradiographs of cement specimens used for leach tests

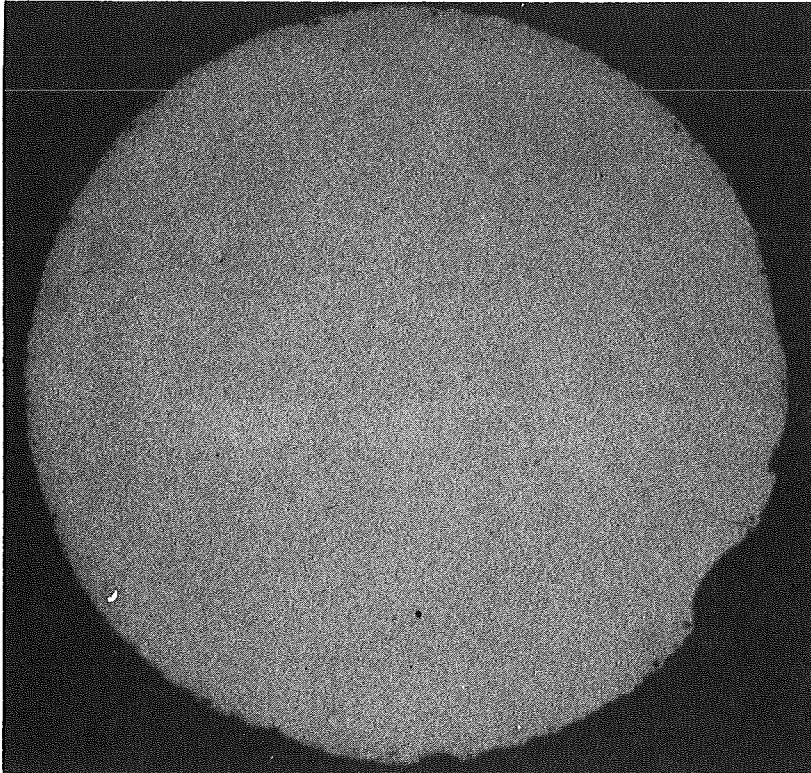


specimen
No A 1/5



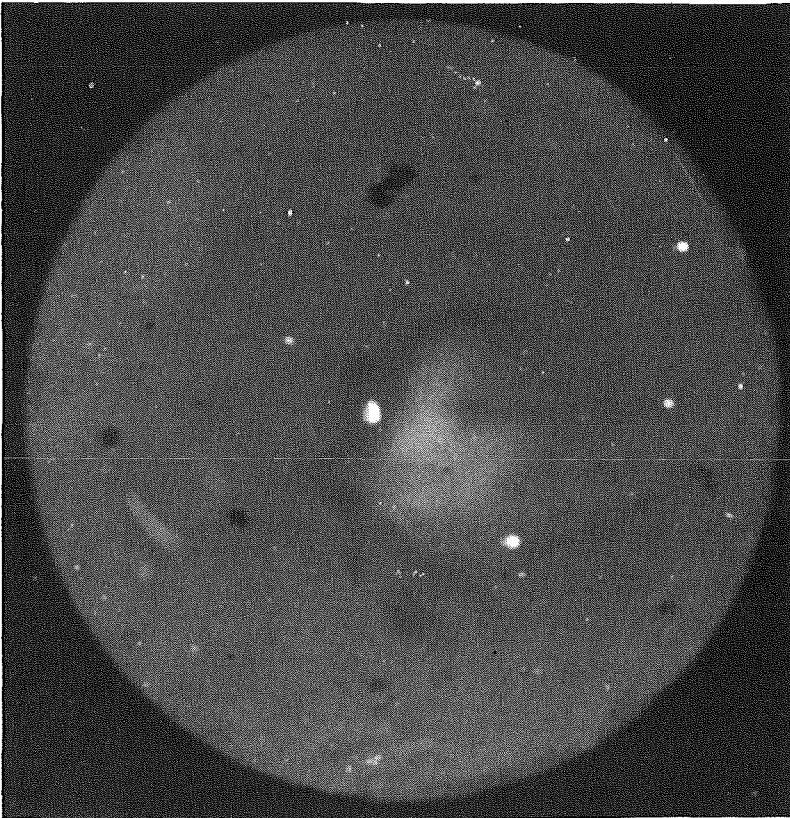
specimen
No A 2/5

Figure 5: Alpha autoradiographs of americium containing borosilicate glass specimens

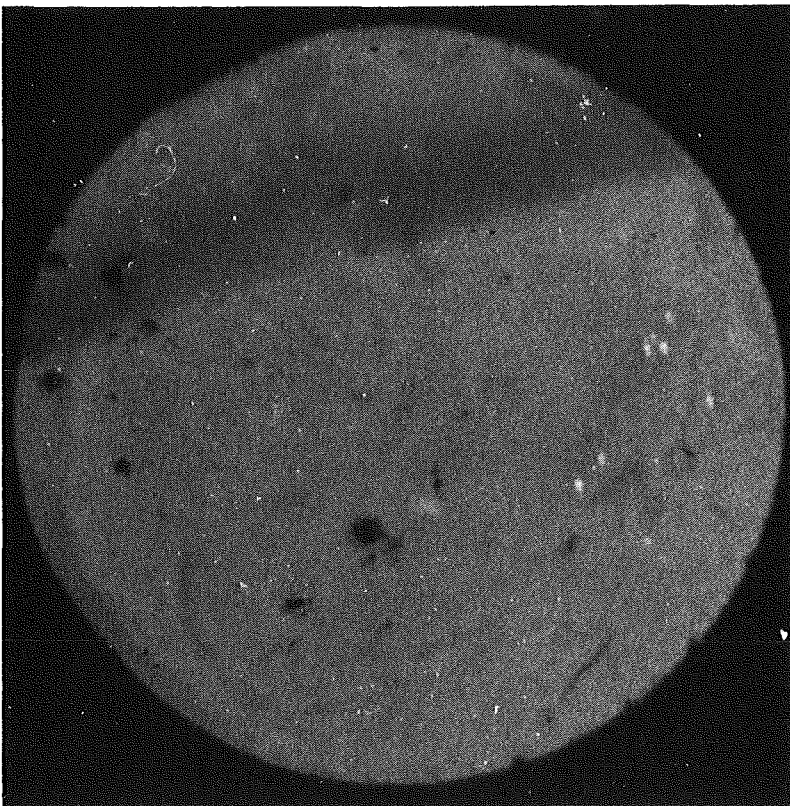


specimen
NO A 3/5

Figure 6: Alpha autoradiograph of americium containing borosilicate glass specimen

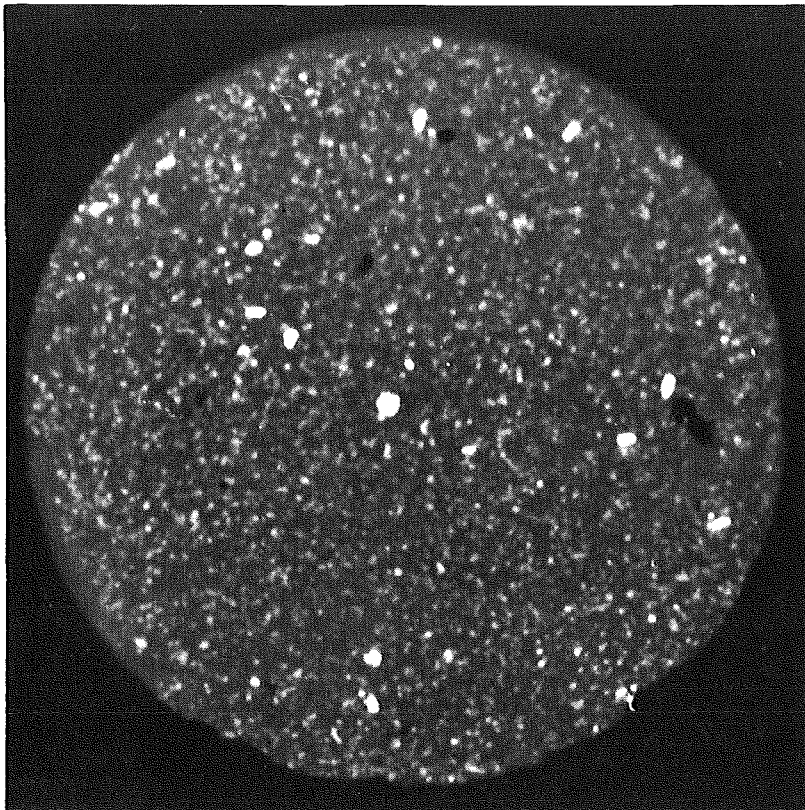


specimen
No P 1/2



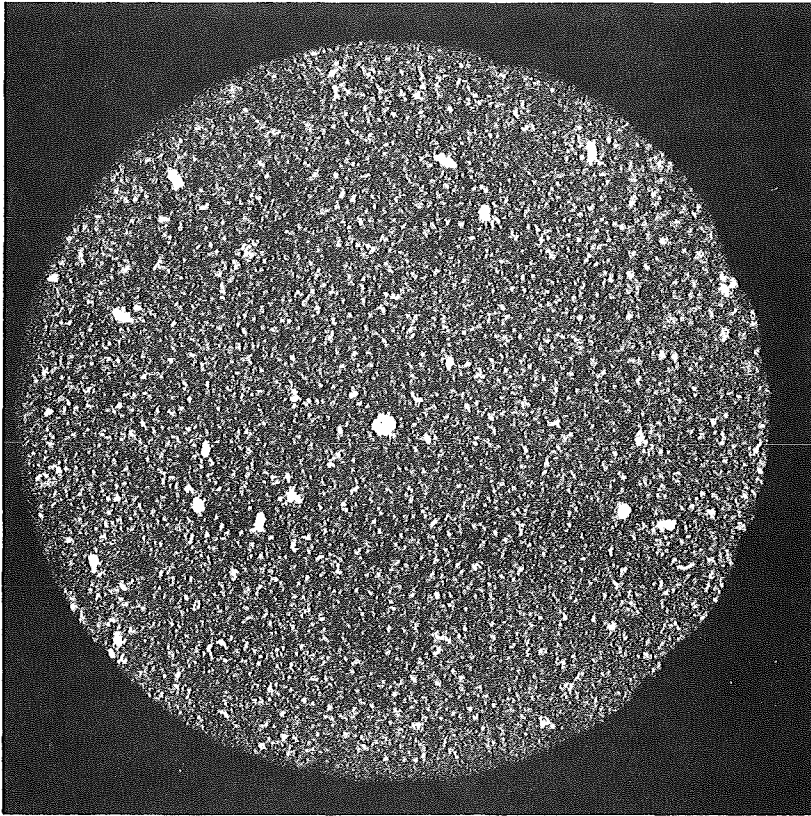
specimen
No P 2/2

Figure 7: Alpha autoradiographs of borosilicate glasses containing 2 wt.% PuO_2

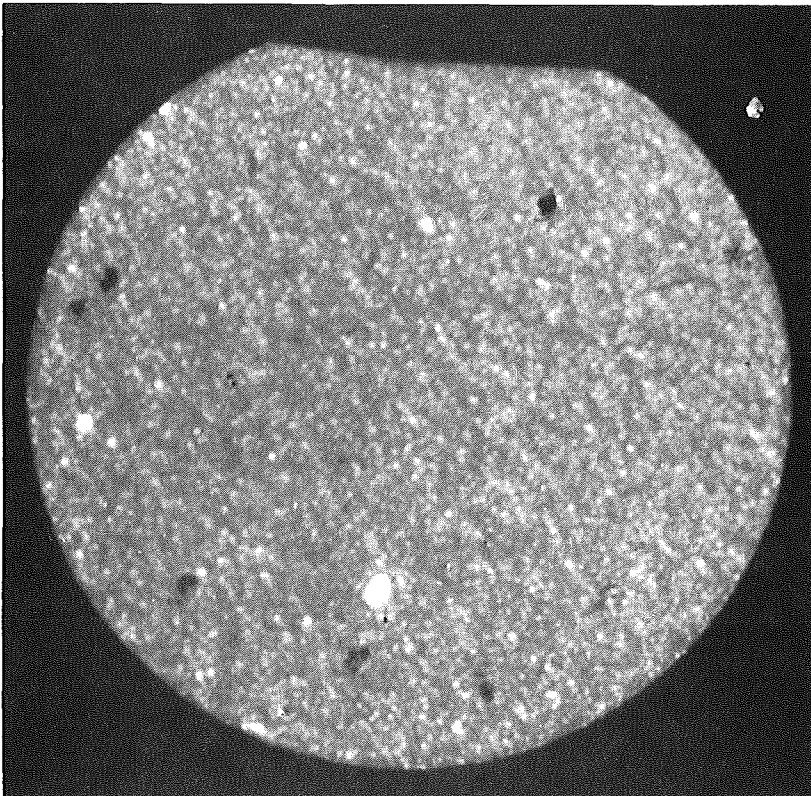


specimen
No P 3/2

Figure 8: Alpha autoradiograph of borosilicate glass containing 2 wt.% PuO_2

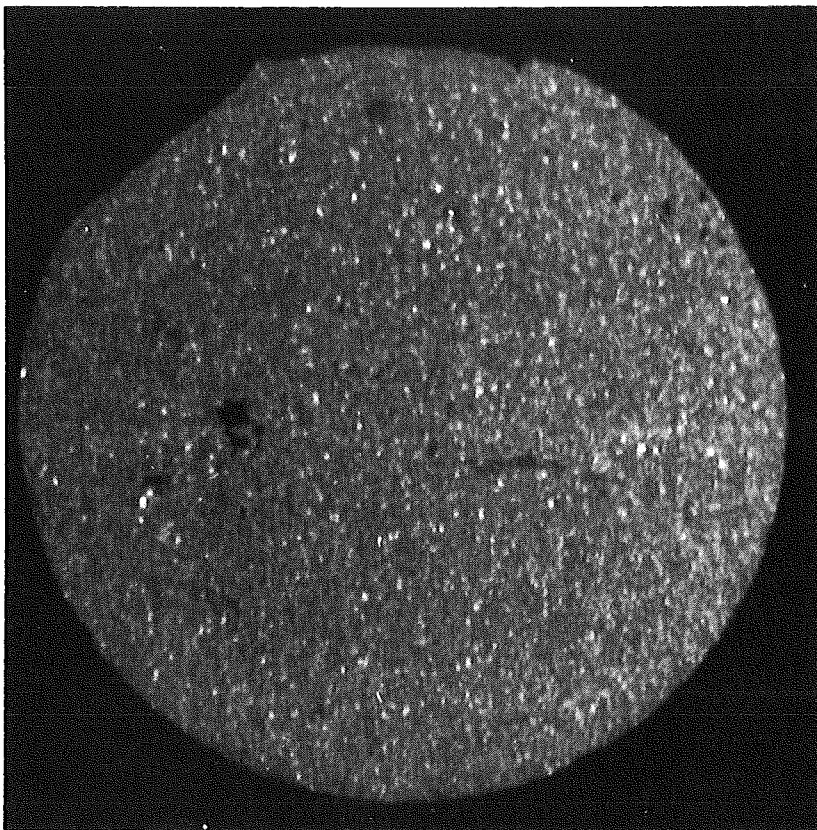


specimen
No P 1/10



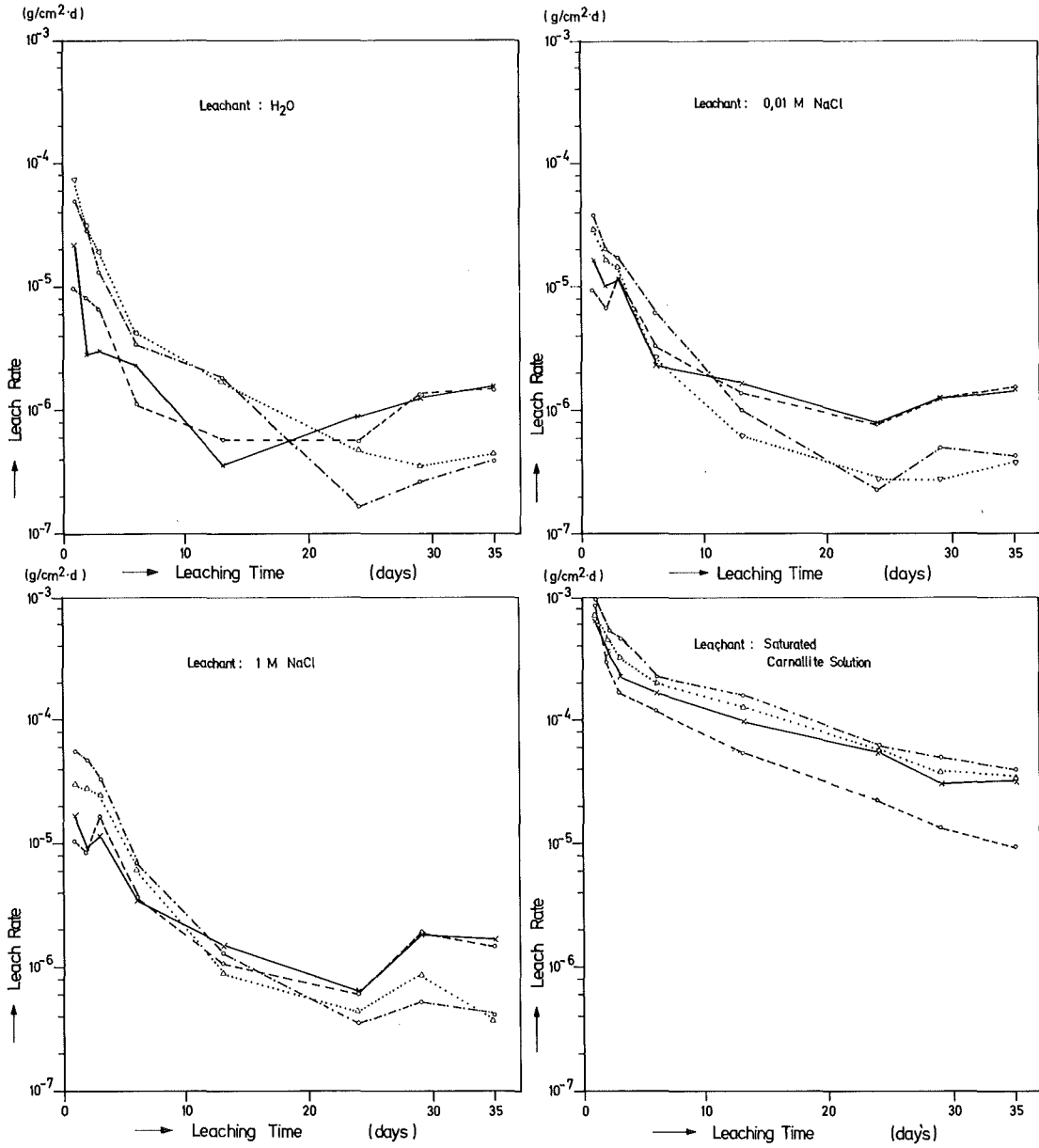
specimen
No P 2/10

Figure 9: Alpha autoradiographs of borosilicate glasses containing 10 wt.% PuO_2



specimen
No P 3/10

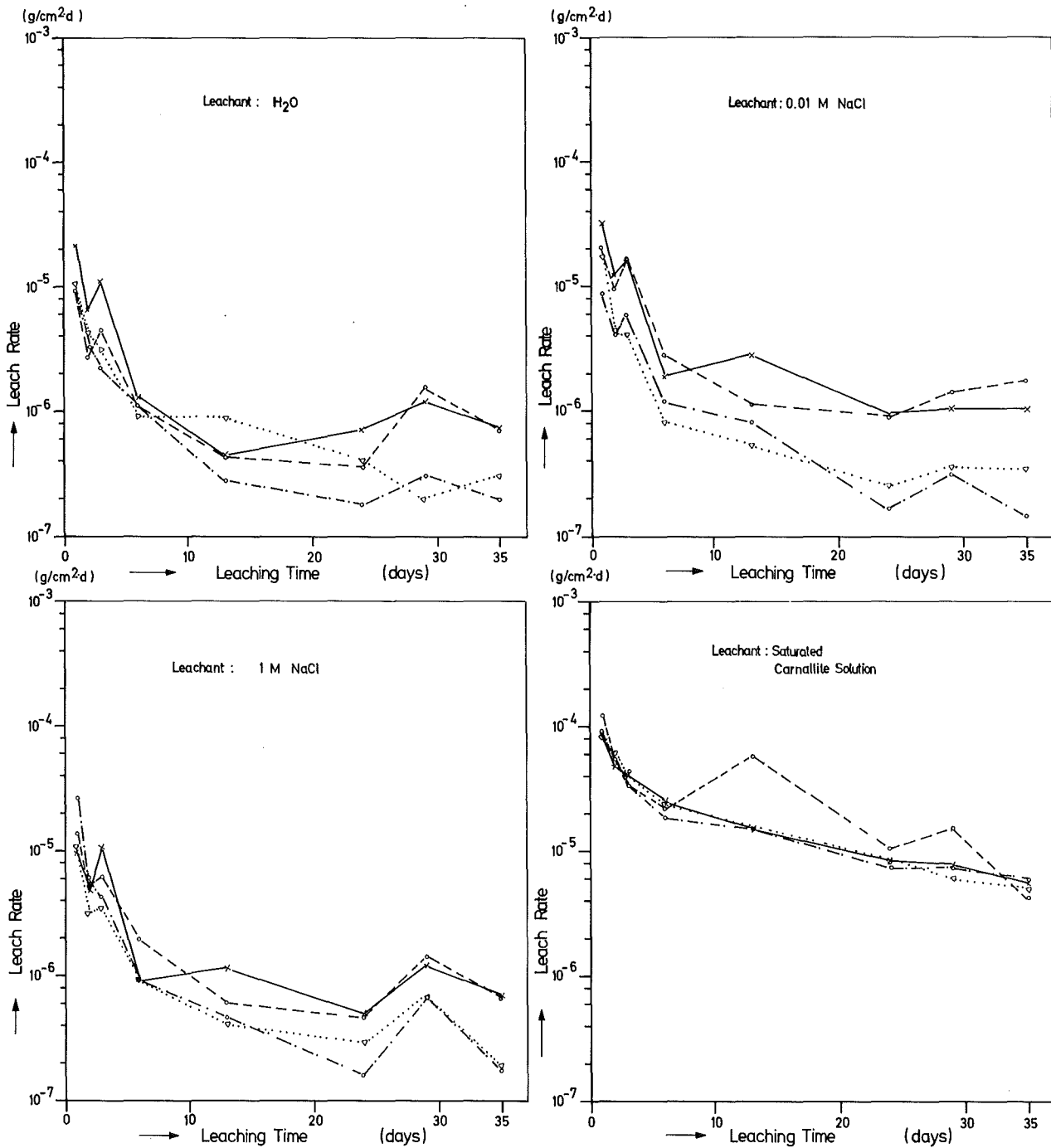
Figure 10: Alpha autoradiograph of borosilicate glass
containing 10 wt.% PuO₂



specimens No:

— C1; ---- C2; -.-.- C5; C6

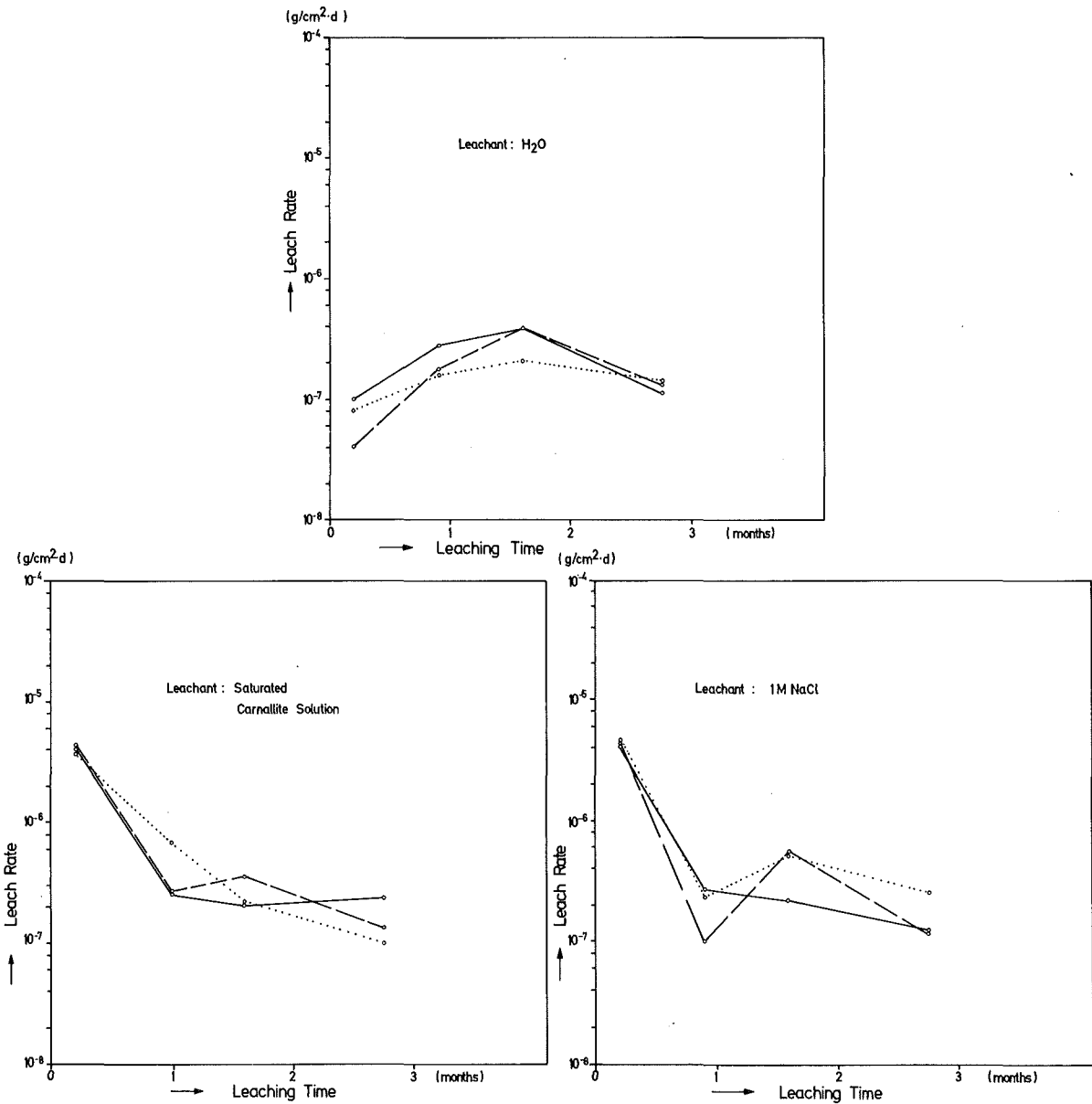
Figure 11: Leach rates for plutonium leached from MLW cement products by different leachants



specimens No:

— C1; ---- C2; -.-.- C5; C6

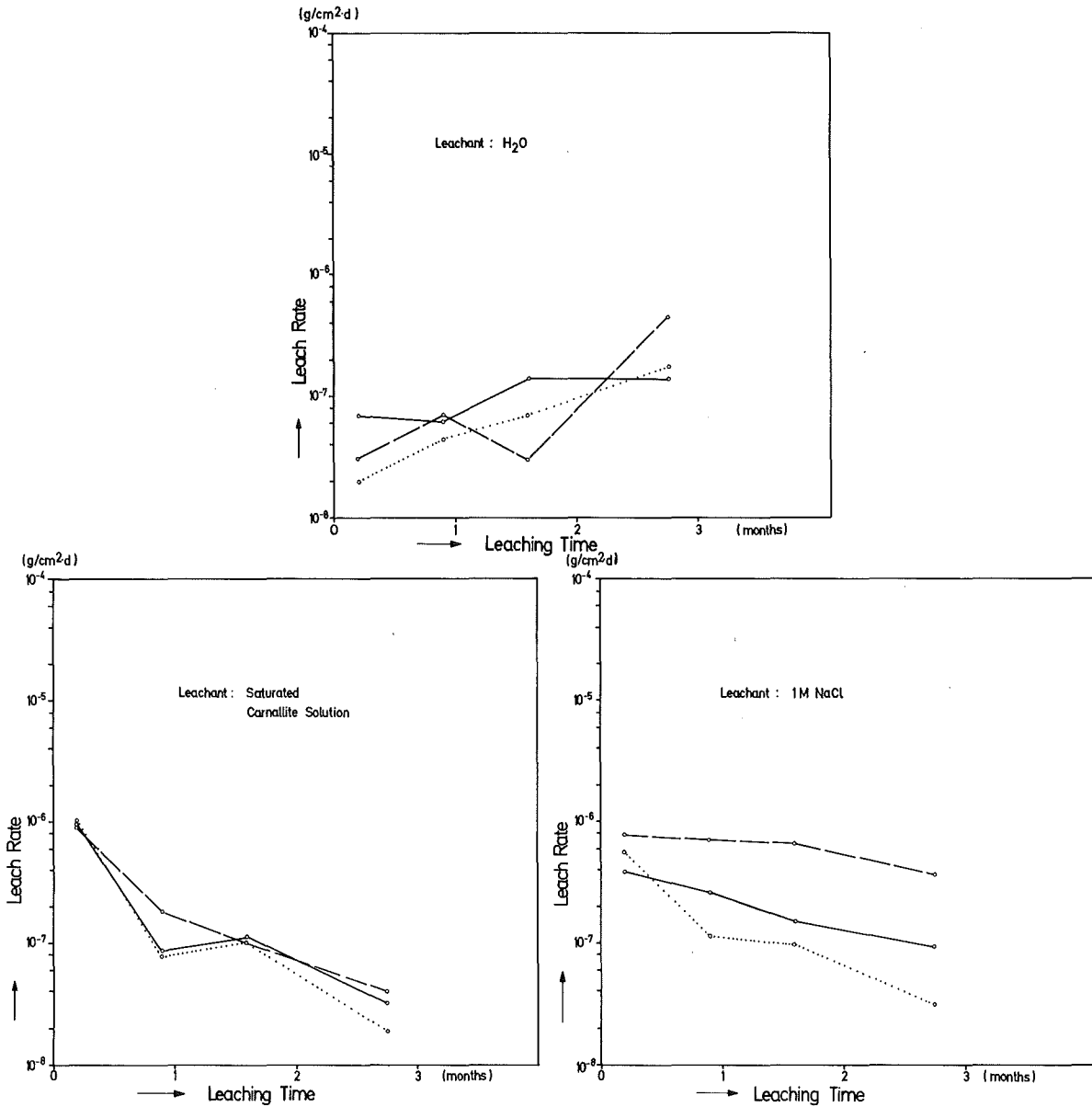
Figure 12: Leach rates for americium leached from MLW cement products by different leachants



specimens No:

—— P 1/2; ---- P 2/2; P 3/2

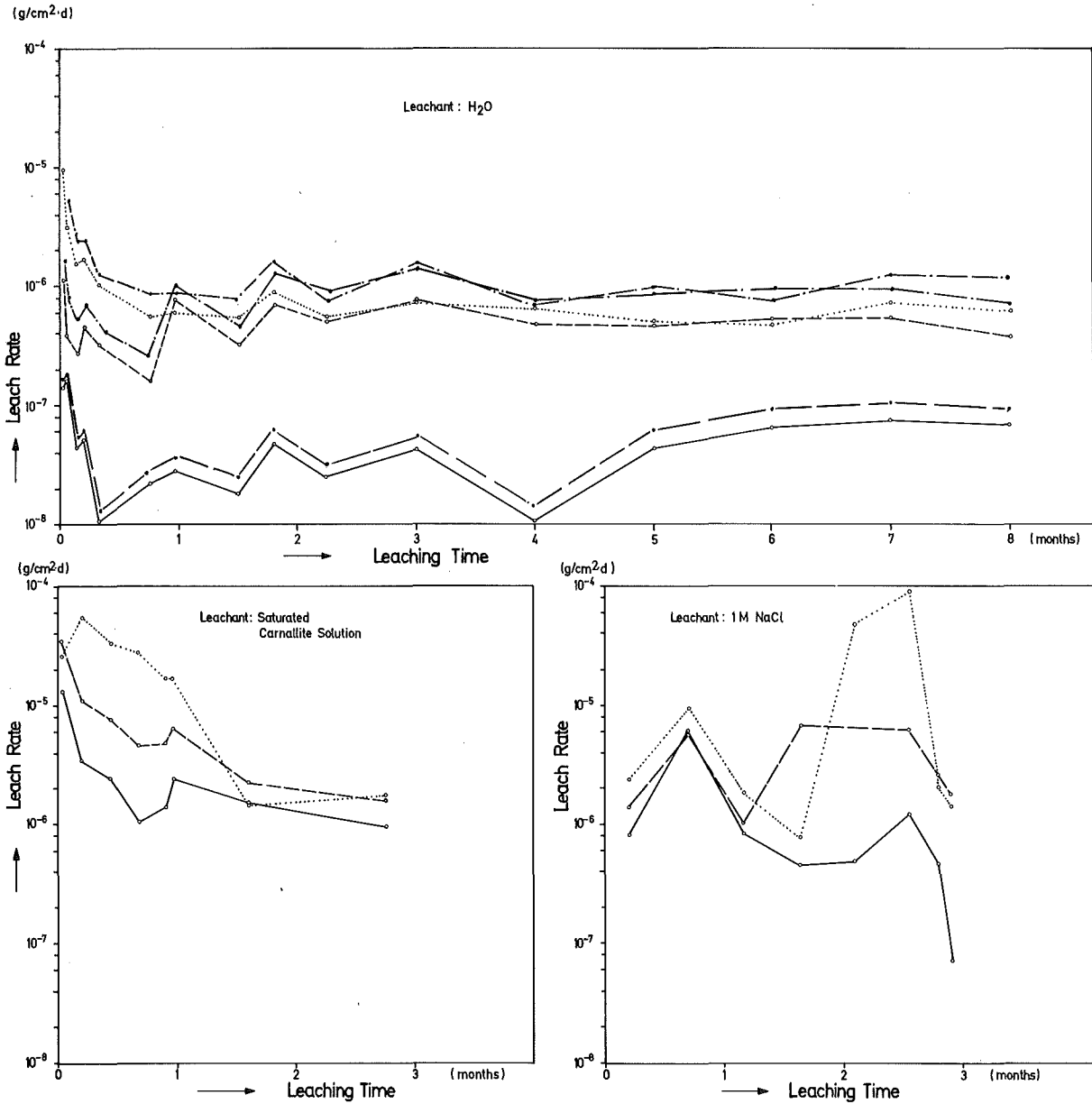
Figure 13: Leach rates for plutonium leached from FLW glasses by different leachants (plutonium content of the glass specimens: 2.0 wt.% PuO₂)



specimens No:

———— P 1/10; ---- P 2/10; P 3/10

Figure 14: Leach rates for plutonium leached from HLW glasses by different leachants (plutonium content of the glass specimens: 10.0 wt.% PuO₂)



specimen No:

Am Cm A 1/5;
 Am Cm A 2/5;
 Am Cm A 3/5

Figure 15: Leach rates for americium leached from HLW glasses by different leachants and curium in demineralized water (americium content of the glass specimens: 4.9 wt.% AmO_2)

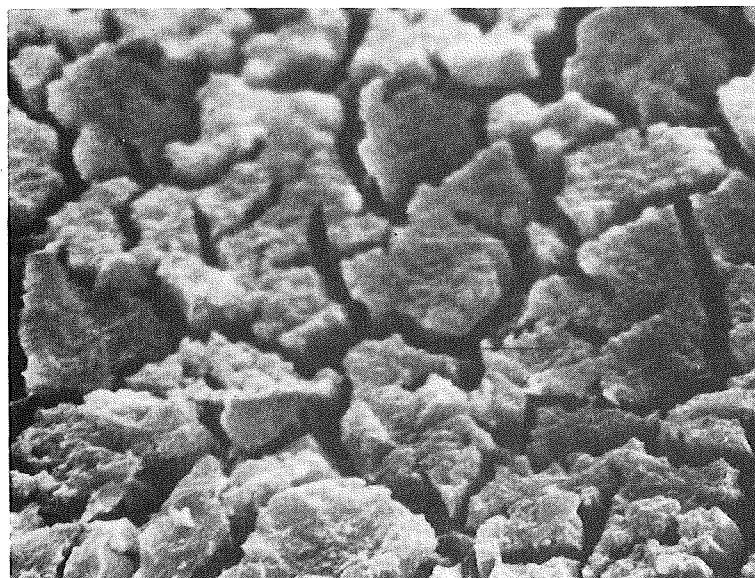
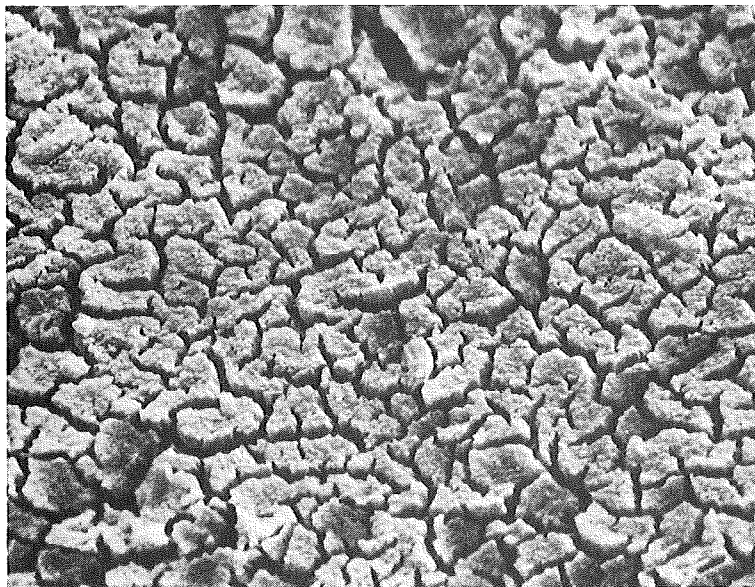
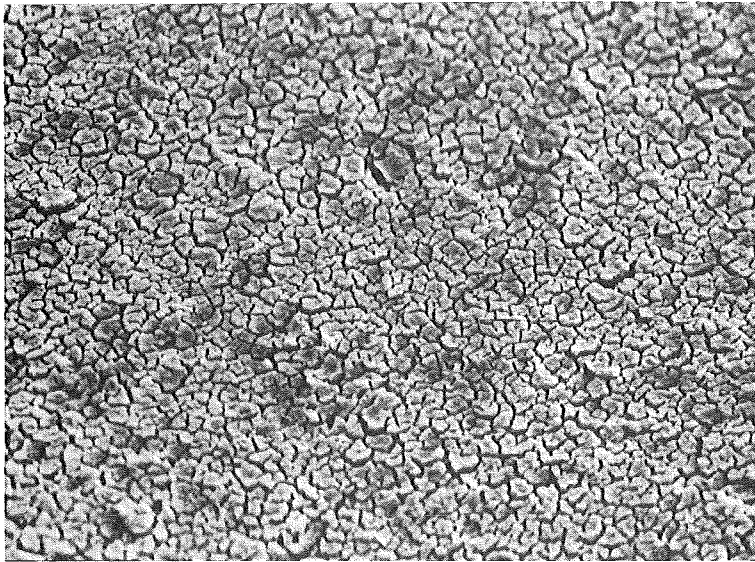


Figure 16: Surface structure of glass specimen No P 1/2 leached with demineralized water (magnifications: 280, 800, 2000)

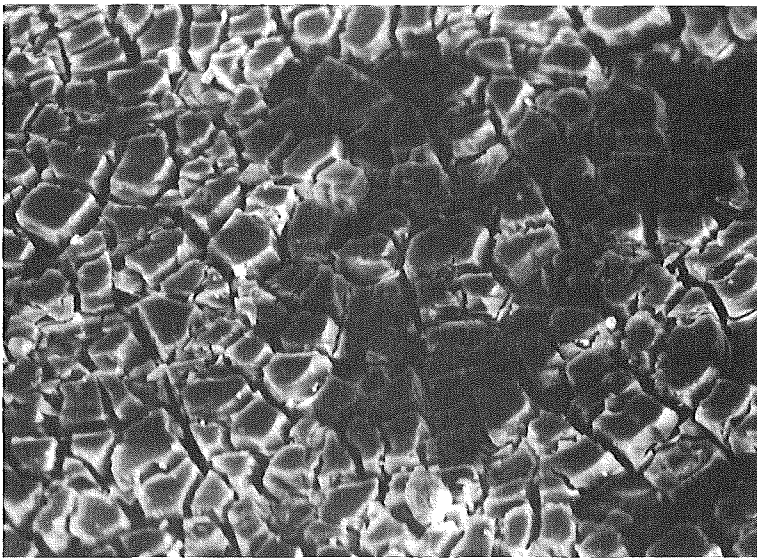
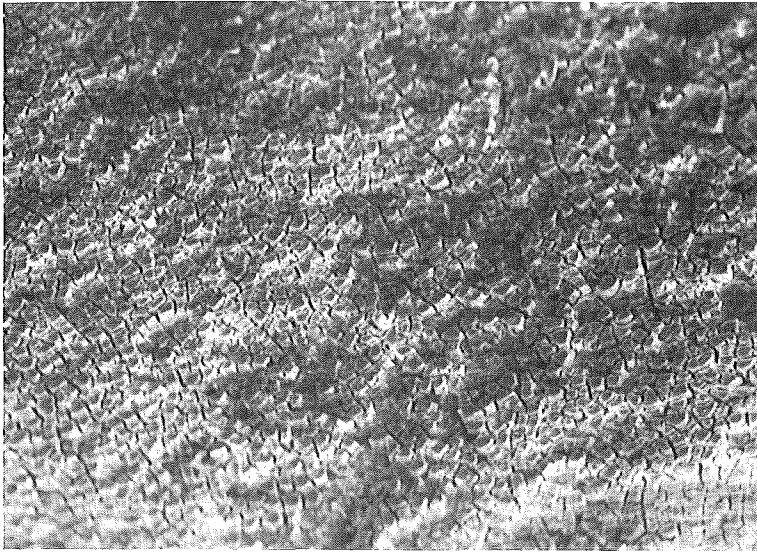


Figure 17: Surface structure of glass specimen No P 1/2
leached with 1 M NaCl solution
(Magnifications: 80, 280, 800)

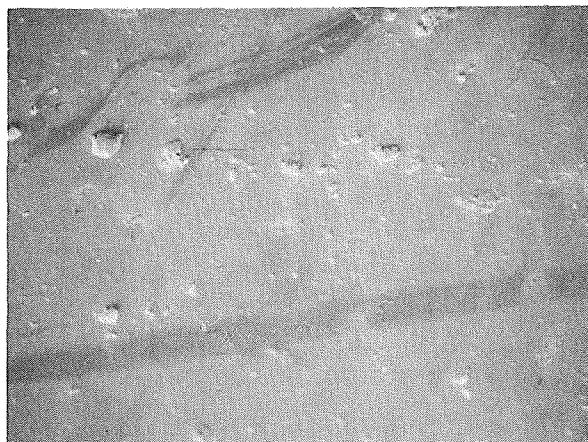
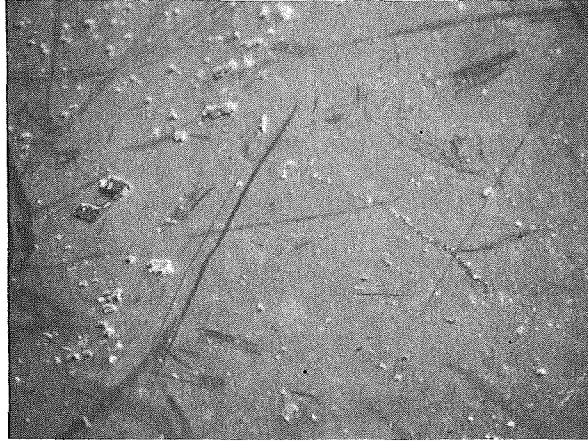


Figure 18: Surface structure of glass specimen No P 1/2 leached with saturated carnallite solution (magnifications: 80, 280, 800)

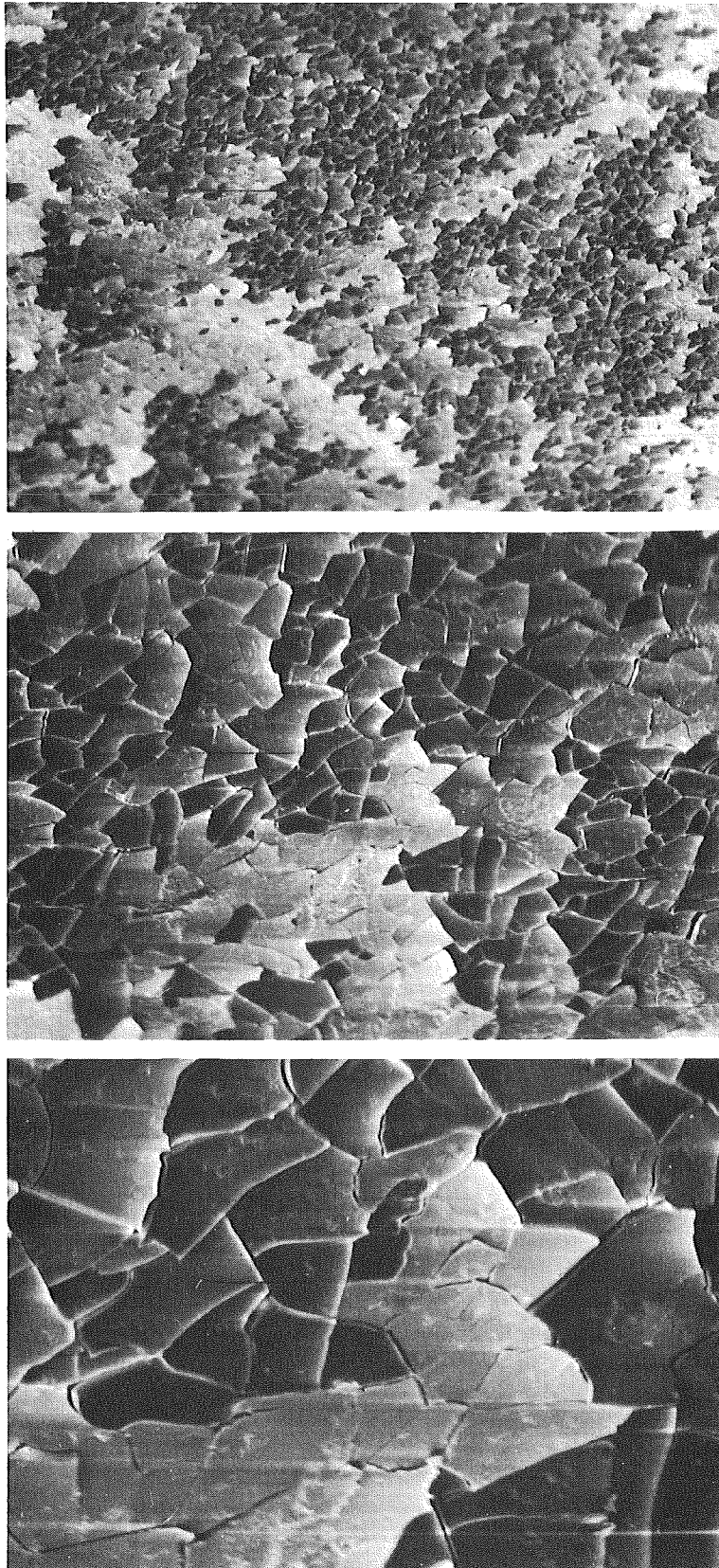


Figure 19: Surface structure of glass specimen
No P 2/2 leached with demineralized
water (magnifications: 80, 280, 800)

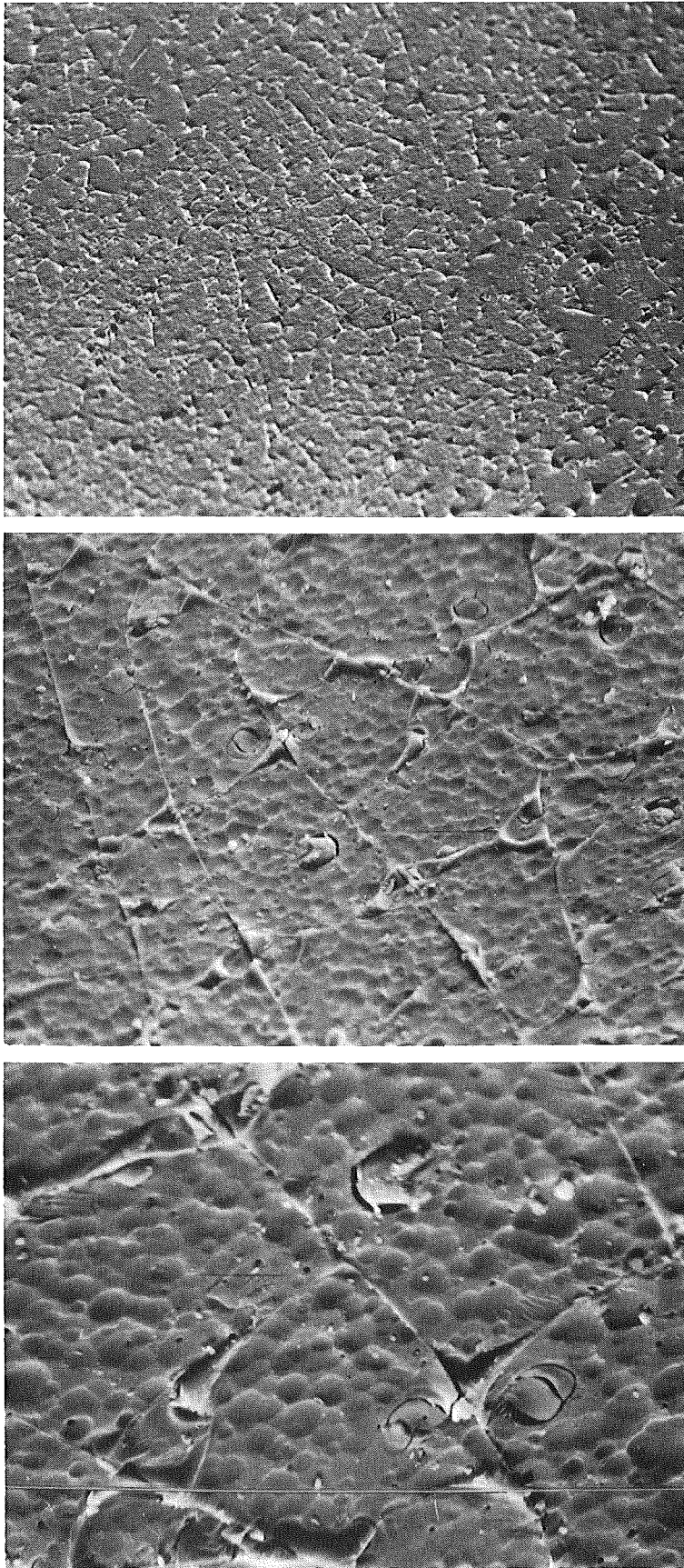


Figure 20: Surface structure of glass specimen No P 2/2
leached with 1 M NaCl solution
(magnifications: 80, 300, 800)

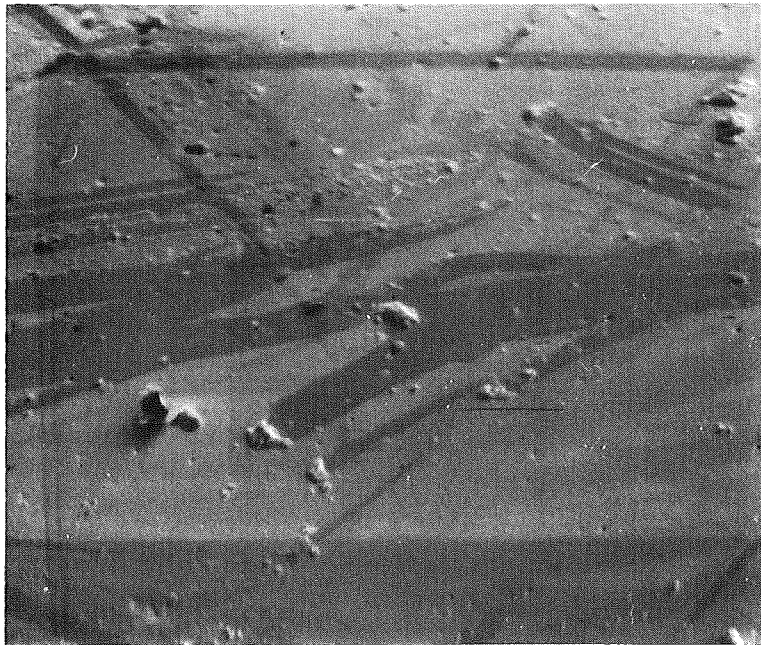
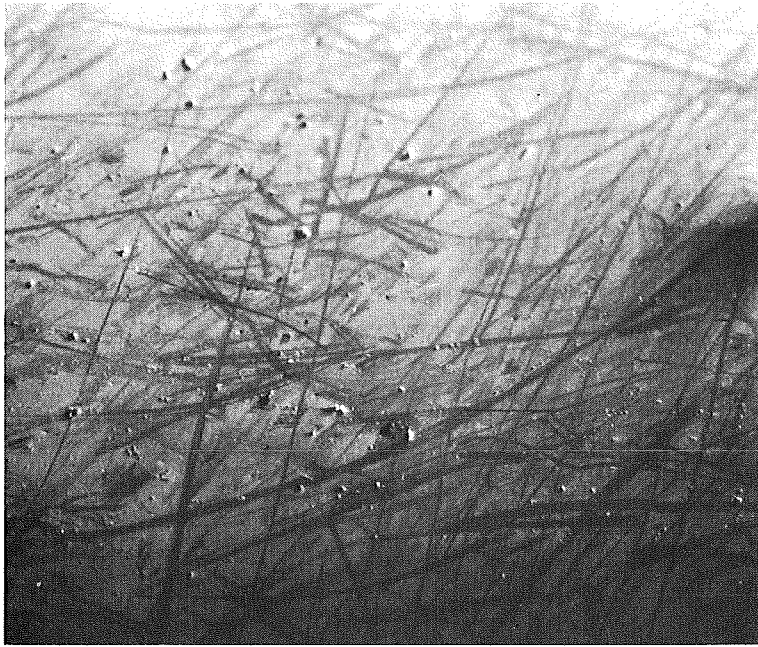


Figure 21: Surface structure of glass specimen No P 2/2 leached with saturated carnallite solution (magnification: 80, 800)

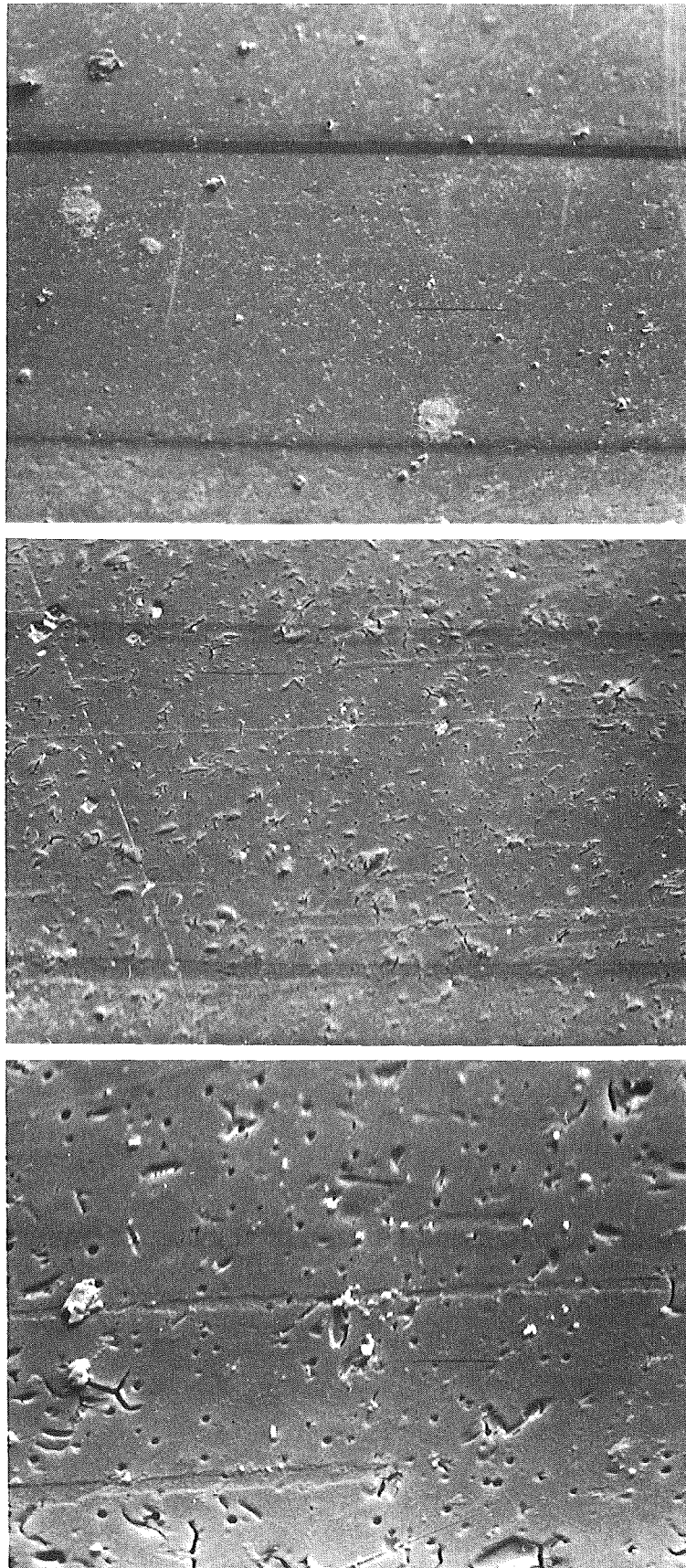


Figure 22: Surface structure of glass specimen No P 3/2 leached with demineralized water (magnifications: 80, 280, 800)

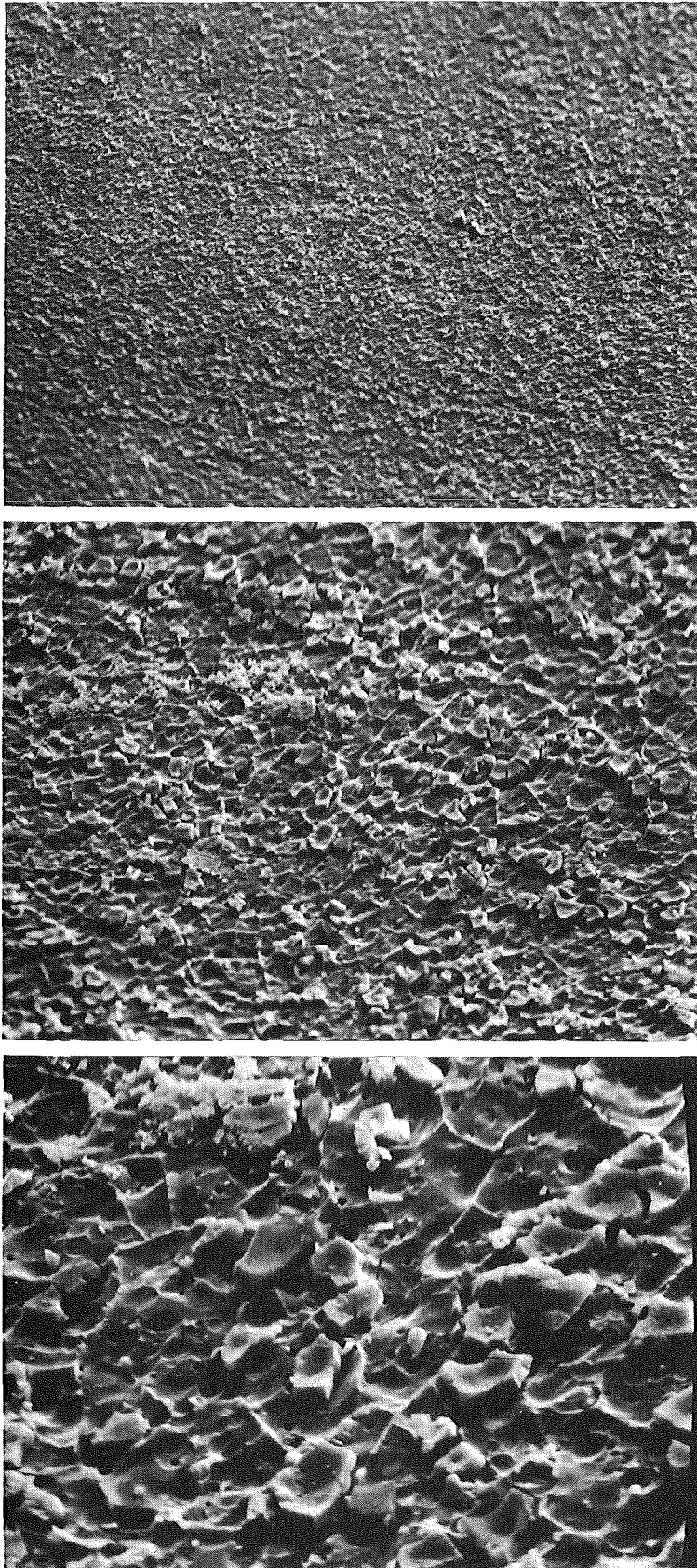


Figure 23: Surface structure of glass specimen No P 3/2
leached with 1 M NaCl solution
(magnifications: 80, 280, 800)

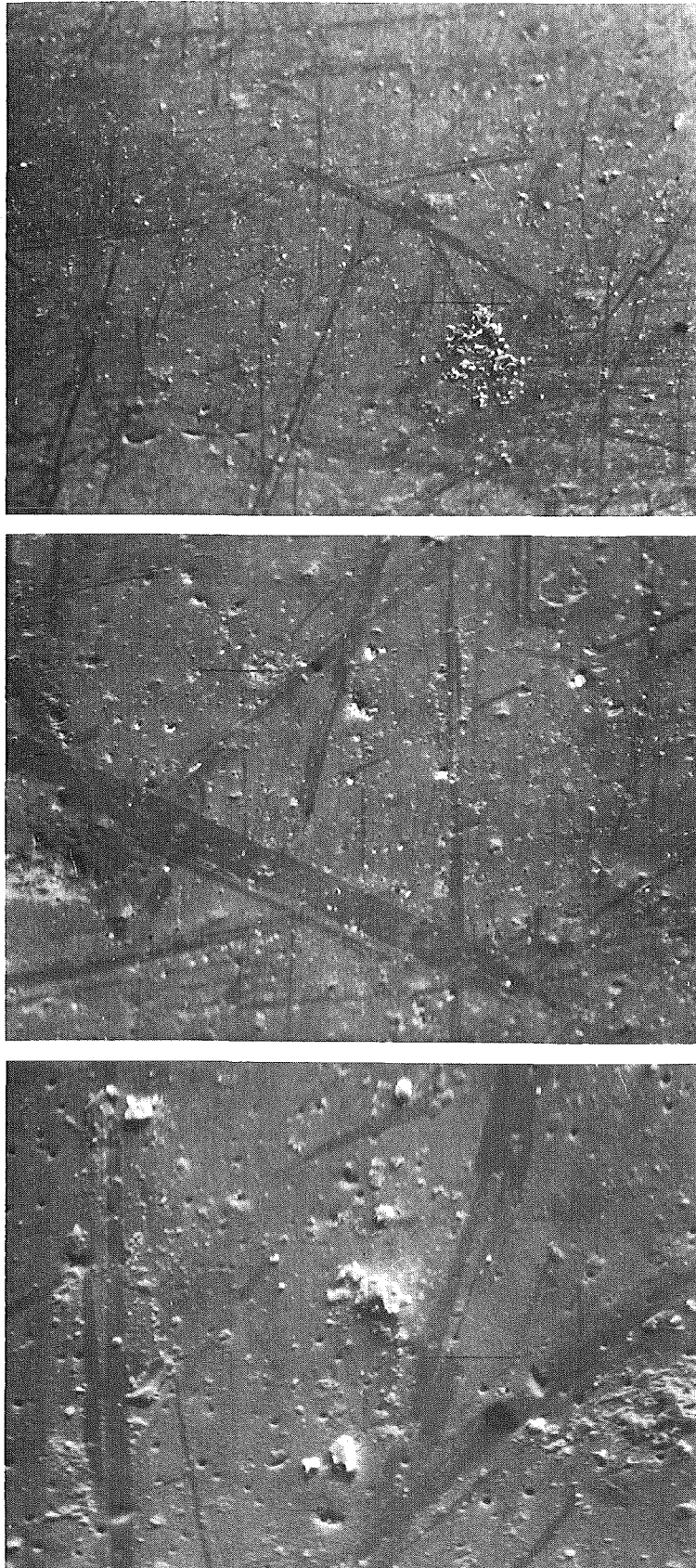


Figure 24: Surface structure of glass specimen No P 3/2 leached with saturated carnallite solution (magnifications: 80, 280, 800)

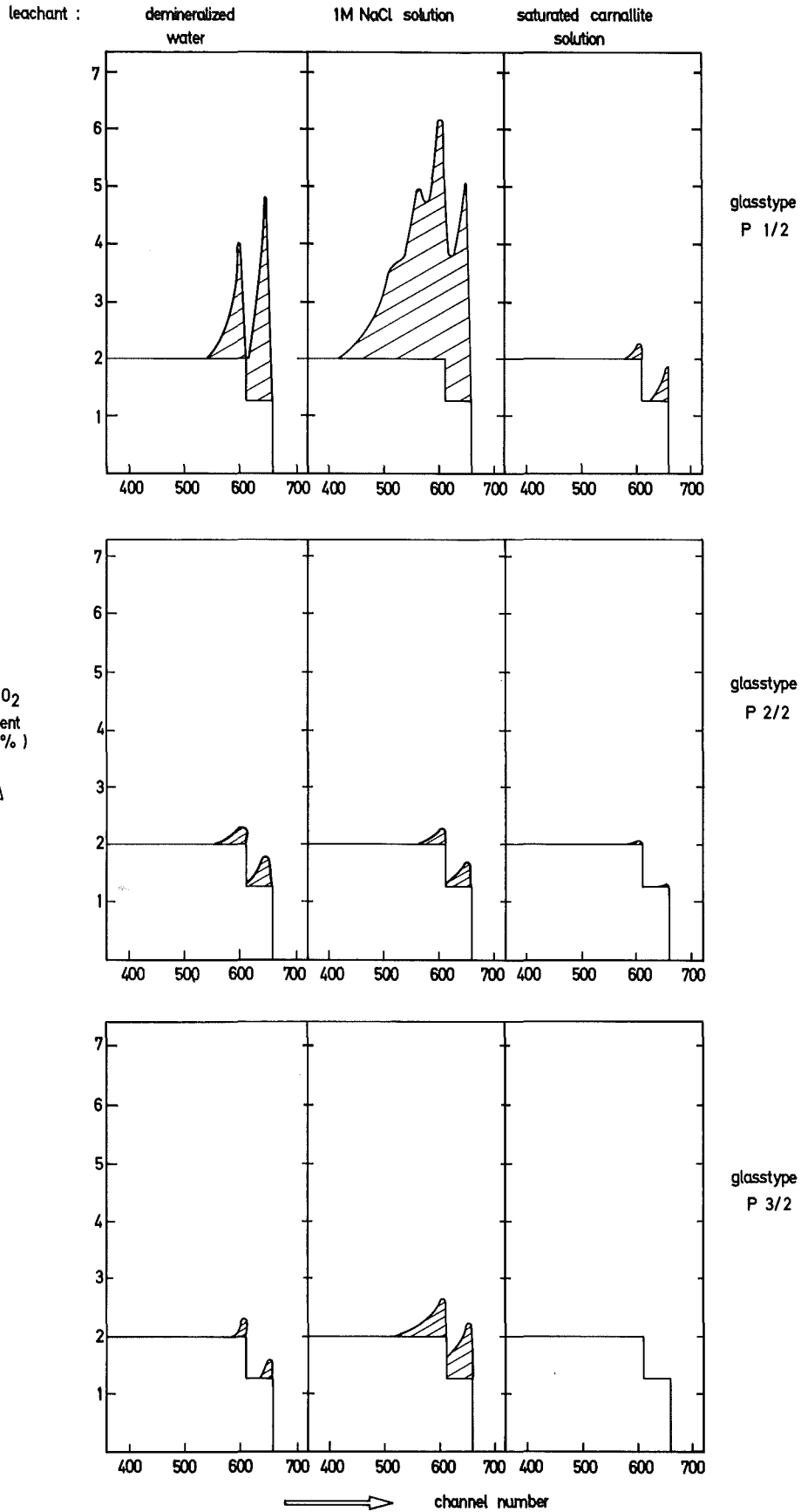


Figure 25: Measured plutonium concentration and plutonium distribution in the surface of leached HLW glass specimens.

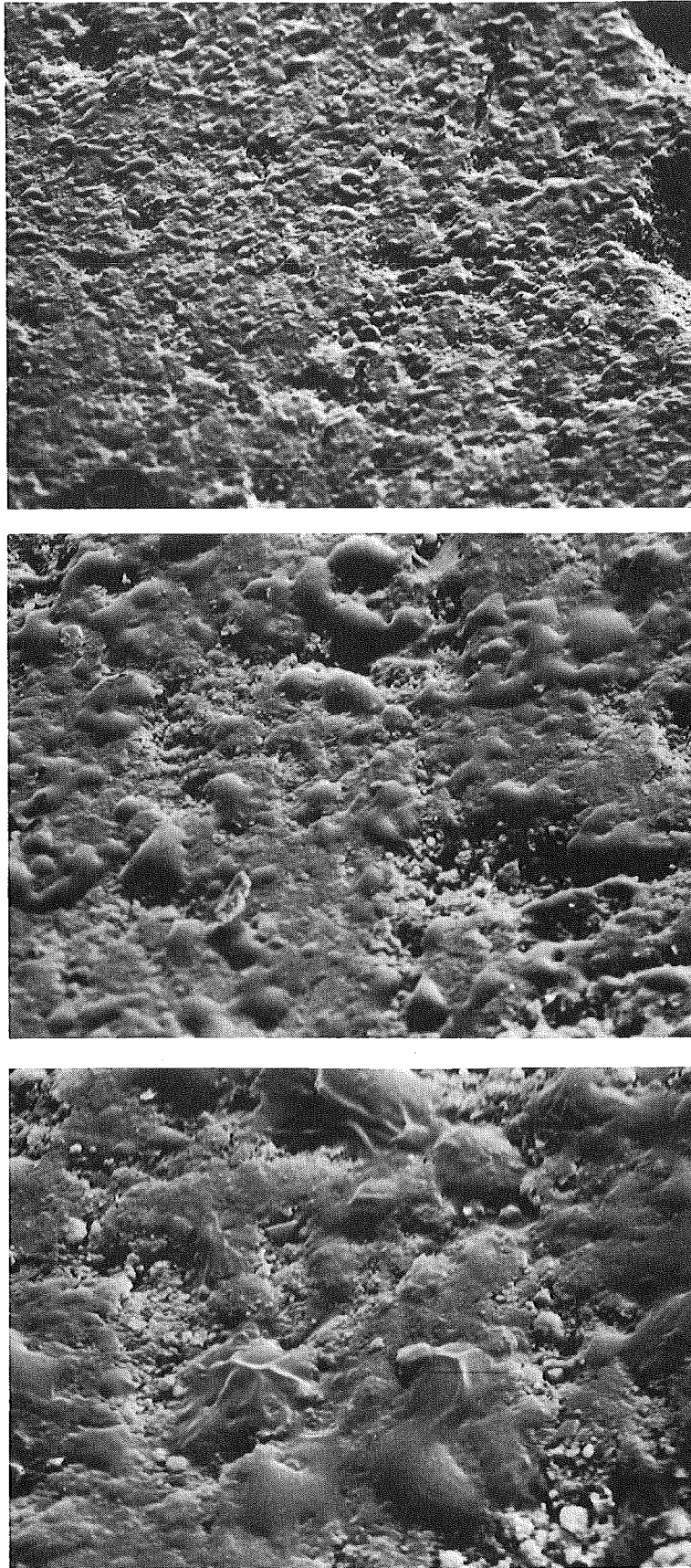


Figure 26: Surface structure of cement specimen
No 5 before leaching
(magnifications: 80, 280, 800)

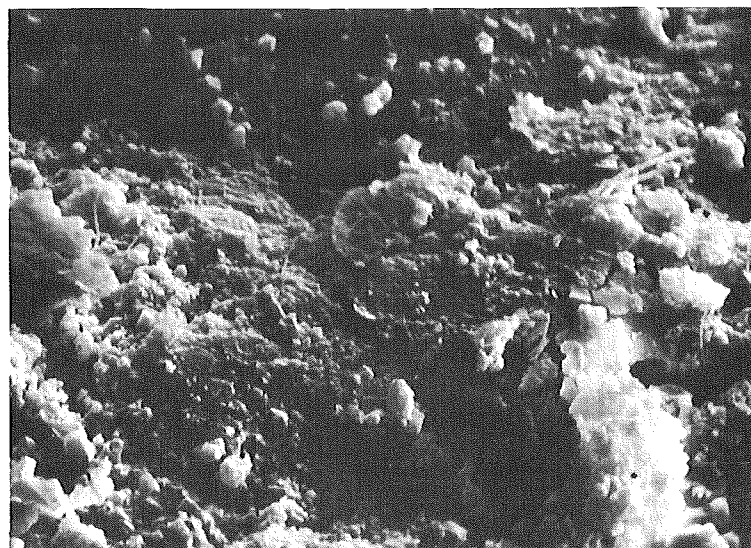
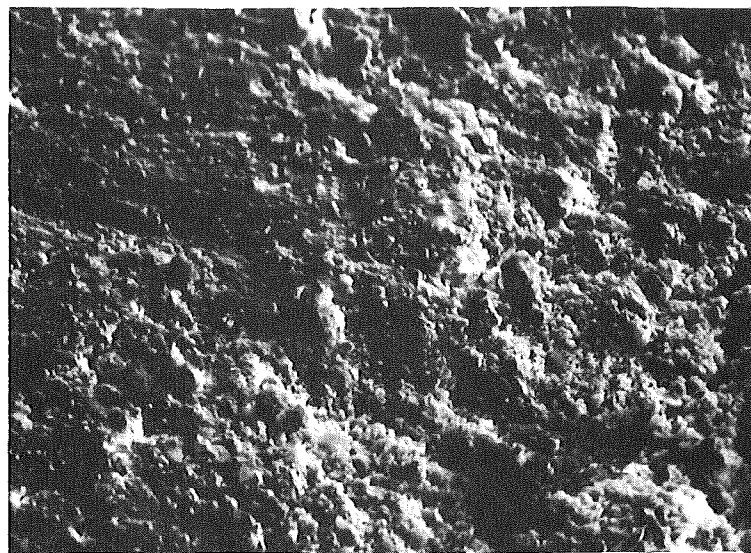


Figure 27: Surface structure of cement specimen No 5 after leaching with demineralized water (magnifications: 80, 280, 800)

<u>List of Figures:</u>	<u>Page</u>
Figure 1: Calculated relative radiotoxicities of fission products and actinides leached from monolithic glass blocks (leach rate $R = 10^{-6} \text{ g/cm}^2 \cdot \text{d}$)	29
Figure 2: Calculated relative radiotoxicities for the total of fission products and actinides leached from monolithic HLW glass blocks (leach rate $R = 10^{-6} \text{ g/cm}^2 \cdot \text{d}$)	30
Figure 3: Alpha autoradiographs of cement specimens used for leach tests	31
Figure 4: Alpha autoradiographs of cement specimens used for leach tests	32
Figure 5: Alpha autoradiographs of americium containing borosilicate glass specimens	33
Figure 6: Alpha autoradiograph of americium containing borosilicate glass specimen	34
Figure 7: Alpha autoradiographs of borosilicate glasses containing 2 wt.% PuO_2	35
Figure 8: Alpha autoradiograph of borosilicate glass containing 2 wt.% PuO_2	36
Figure 9: Alpha autoradiographs of borosilicate glass containing 10 wt.% PuO_2	37
Figure 10: Alpha autoradiograph of borosilicate glass containing 10 wt.% PuO_2	38

	<u>Page</u>
Figure 11: Leach rates for plutonium leached from MLW cement products by different leachants	39
Figure 12: Leach rates for americium leached from MLW cement products by different leachants	40
Figure 13: Leach rates for plutonium leached from HLW glasses by different leachants (plutonium content of the glass specimens: 2.0 wt.% PuO ₂)	41
Figure 14: Leach rates for plutonium leached from HLW glasses by different leachants (plutonium content of the glass specimens: 10.0 wt.% PuO ₂)	42
Figure 15: Leach rates for americium leached from HLW glasses by different leachants (americium content of the glass specimens: 4.9 wt.% AmO ₂)	43
Figure 16: Surface structure of glass specimen No P 1/2 leached with demineralized water (magnifications: 280, 800, 2000)	44
Figure 17: Surface structure of glass specimen No P 1/2 leached with 1 M NaCl solution (magnifications: 80, 280, 800)	45
Figure 18: Surface structure of glass specimen No P 1/2 leached with saturated carnallite solution (magnifications: 80, 280, 800)	46

	<u>Page</u>
Figure 19: Surface structure of glass specimen No P 2/2 leached with demineralized water (magnifications: 80, 280, 800)	47
Figure 20: Surface structure of glass specimen No P 2/2 leached with 1 M NaCl solution (magnifications: 80, 300, 800)	48
Figure 21: Surface structure of glass specimen No P 2/2 leached with saturated carnallite solution (magnifications: 80, 800)	49
Figure 22: Surface structure of glass specimen No P 3/2 leached with demineralized water (magnifications: 80, 280, 800)	50
Figure 23: Surface structure of glass specimen No P 3/2 leached with 1 M NaCl solution (magnifications: 80, 280, 800)	51
Figure 24: Surface structure of glass specimen No P 3/2 leached with saturated carnallite solution (magnifications: 80, 280, 800)	52
Figure 25: Measured plutonium concentration and plutonium distribution in the surface of leached HLW glass specimens	53
Figure 26: Surface structure of cement specimen No C 5 before leaching (magnifications: 80, 280, 800)	54
Figure 27: Surface structure of cement specimen No C 5 after leaching with demineralized water (magnifications: 80, 280, 800)	55

References

- {1} K. Scheffler, U. Riege, W. Hild, A.T. Jakubick
Zur Problematik der sicheren Beseitigung α -haltiger
Abfälle aus Wiederaufarbeitung und Brennelement-
fertigung am Beispiel des Langzeitverhaltens hoch-
aktiver Gläser
KFK-2170 (Juli 1975)
- {2} Siting of Fuel Reprocessing Plants and Waste
Management Facilities
ORNL-4451 (Juli 1970)
- {3} Hj. Matzke
On the Energy Loss of α -Particles in the Surface of
Leached Glass (1977)
unpublished
- {4} B.A. Brice, M. Halwer
A Differential Refractometer
Journal of the Optical Society of America 41, 12
p.p. 1033-37 (December, 1951)
- {5} B.A. Brice, M. Halwer, R. Speiser
Photoelectric Light-Scattering Photometer for Determining
High Molecular Weights
Journal of the Optical Society of America '40, 11
p.p. 768-78 (November, 1950)
- {6} K.P. Louwrier, T. Steemers
Study of Hydrolysis of Cerium (IV) in Perchlorate
Solution by Light-Scattering
Inorg. Nucl. Chem. Letters 12, pp. 195-89 (1976)

- {7} Verordnung über den Schutz vor Schäden durch ionisierende Strahlen (Strahlenschutzverordnung) in der Fassung vom 13.10.1976, § 46 Abs. 4, Anlage IV 1 Spalte 6 (Bonn, 20. Oktober 1976)